AIMS Mathematics, 9(11): 31898–31925.
DOI: 10.3934/math.20241533
Received: 28 August 2024
Revised: 21 October 2024
Accepted: 21 October 2024
Published: 11 November 2024

https://www.aimspress.com/journal/Math

Research article

Numerical analysis of the fractional nonlinear waves of fifth-order KdV and Kawahara equations under Caputo operator

Musawa Yahya Almusawa* **and Hassan Almusawa**

Department of Mathematics, Faculty of Science, Jazan University, P.O. Box 2097, Jazan 45142, Kingdom of Saudi Arabia; haalmusawa@jazanu.edu.sa

* **Correspondence:** Email: malmusawi@jazanu.edu.sa.

Abstract: This study delved into the analytical investigation of two significant nonlinear partial differential equations, namely the fractional Kawahara equation and fifth-order Korteweg-De Vries (KdV) equations, utilizing advanced analytical techniques: the Aboodh residual power series method and the Aboodh transform iterative method. Both equations were paramount in various fields of applied mathematics and physics due to their ability to describe diverse nonlinear wave phenomena. Here, we explored using the Aboodh methods to efficiently solve these equations under the framework of the Caputo operator. Through rigorous analysis and computational simulations, we demonstrated the efficacy of the proposed methods in providing accurate and insightful solutions to the time fractional Kawahara equation and fifth-order KdV equations. Our study advanced the understanding of nonlinear wave dynamics governed by fractional calculus, offering valuable insights and analytical tools for tackling complex mathematical models in diverse scientific and engineering applications.

Keywords: fractional Kawahara equation; fifth-order KdV equations; Aboodh residual power series method; Aboodh transform iteration method; Caputo operator
Mathematics Subject Classification: 34G20, 35A20, 35A22, 35R11

1. Introduction

Many complicated structures' memory and natural features may be realized using fractional calculus (FC), which studies integrals and derivatives of fractional orders [1, 2]. Many recent FC applications have included analyzing the dynamics of large-scale physical events by converting derivatives and integrals from classical to non-integer order. Many branches of engineering and the physical sciences use it, including electric circuits, mathematical biology, control theory, robotics, viscoelasticity, flow models, relaxation, and signal processing [3, 4]. Numerous mysterious ideas have been refined via the study of fractional calculus, for example, logistic regression, Malthusian growth,

and blood alcohol concentration, all of which have shown that fractional operators outperform integer-order operators [5, 6].

Derivatives of fractional order such as Riemann-Liouville, Atangana Baleanu, Caputo, Hilfer, Grunwald-Letnikov, Caputo Fabrizio, and Riemann-Liouville are among the numerous that have recently been proposed [7, 8]. Since all fractional derivatives may be reduced in Caputo's meaning with minor parametric adjustments, the fractional derivative of Caputo is the essential principle of FC to investigate fractional differential equations (FDEs). Caputo's operator, which has numerous applications to model various physical models, possesses a power-law kernel. To address this difficulty, the alternative fractional differential operator [9] was developed, which consists of a Mittag-Leffler kernel and an exponentially decaying kernel. Caputo-Fabrizio (CF) and Atangana-Baleanu are operators characterized by their non-singular kernels. These operators have been widely applied in analyzing diverse problem classes, including but not limited to biology, economics, geophysics, and bioengineering [10].

Korteweg and de Vries introduced the KdV equation in 1895 to formulate a model for Russell's soliton phenomenon, encompassing water waves of long and small amplitude. Solitons are classified as stable solitary waves, signifying their particle-like nature [11]. Various applied disciplines, including plasma physics, fluid dynamics, quantum mechanics, and optics, implement the KdV equations [12]. Particle physics has employed the fifth-order KdV equations to analyze many nonlinear phenomena [13]. Its function in the propagation of waves is crucial [14]. The authors find third-order and fifth-order dispersive terms in the KdV form equation pertinent to the magneto-acoustic wave problem. Furthermore, these dispersive terms manifest themselves in the vicinity of critical angle propagation [15]. An electrically conducting fluid, plasma is also dynamic and quasi-neutral. Ions, electrons, and neutral particles comprise it. Due to the electrical conductivity exhibited by plasma, it includes both electric and magnetic regions. The variety of particles and regions supports diverse types of plasma waves. A magnetic lock is a less longitudinal ion dispersion. In the low magnetic field range, the magneto-acoustic wave exhibits characteristics of an ion acoustic wave [16, 17]. However, at low temperatures, it transforms into an Alfven wave.

Equivalent to the general model for the investigation of magnetic characteristics of acoustic waves with surface tension is the fifth order of KdV. According to a recent investigation [18, 19], the solutions to the equation above concerning traveling waves persist beyond infinity. The following are two widely recognized types of fifth-order KdV equations [20, 21]:

$$D_{\Omega}^{p}\eta(\epsilon,\Omega) - \frac{\partial^5\eta(\epsilon,\Omega)}{\partial\epsilon^5} + \eta(\epsilon,\Omega)\frac{\partial^3\eta(\epsilon,\Omega)}{\partial\epsilon^3} + \eta(\epsilon,\Omega)\frac{\partial\eta(\epsilon,\Omega)}{\partial\epsilon} = 0, \;\; 0 < p \leq 1. \tag{1.1}$$

$$D_{\Omega}^{p}\eta(\epsilon,\Omega) + \frac{\partial^5\eta(\epsilon,\Omega)}{\partial\epsilon^5} - \eta(\epsilon,\Omega)\frac{\partial^3\eta(\epsilon,\Omega)}{\partial\epsilon^3} + \eta(\epsilon,\Omega)\frac{\partial\eta(\epsilon,\Omega)}{\partial\epsilon} = 0, \;\; 0 < p \leq 1. \tag{1.2}$$

Here, Eqs (1.1) and (1.2) are called the Kawahara and KdV equation of fifth-order, respectively. The extreme nonlinearity of these mathematical models makes it difficult to find suitable analytical methods. Researchers have developed and implemented several techniques for solving nonlinear and linear equations of KdV in the past ten years. These techniques include the variational iteration method [21], the multi-symplectic method [22], He's homotopy perturbation method [23], and the Exp-function method [24].

Omar Abu Arqub established residual power series method (RPSM) in 2013 [25]. It is created by merging the residual error function with the Taylor series. According to [26], an infinite convergence series solves differential equations (DEs). The development of novel RPSM algorithms has been prompted by several DEs, including KdV Burger's equation, fuzzy DEs, Boussinesq DEs, and numerous others [27, 28]. The goal of these algorithms is to provide efficient and accurate estimates.

A novel strategy for solving FDEs was established by integrating two effective methods. Some approaches that fall into these categories include those that use the natural transform [29], the Laplace transform with RPSM [30], and the homotopy perturbation method [31]. In this work, we used a novel combination method known as the Abdooh residual power series method (ARPSM) to discover approximation and precise solutions for time-fractional nonlinear partial differential equations (PDEs). This innovative method is significant because it combines the Aboodh transform technique with the RPSM [32, 33].

The computing effort and complexity needed are significant issues with the previously mentioned approaches. Our suggested Aboodh transform iterative method (ATIM) [34] is this work's unique aspect that solves the Kawahara and KdV equations of fractional order. By integrating the Aboodh transform with the new iterative technique, this strategy significantly reduces the computing effort and complexity required. According to [35,36], the suggested approach yields a convergent series solution.

The ARPSM and the ATIM are the two most straightforward approaches to solving fractional DEs. These methods fully and immediately explain the symbolic terms used in analytical solutions and offer numerical solutions to PDEs. This paper assesses ATIM and ARPSM's efficacy in solving the fifth-order KdV and Kawahara equations.

The fifth-order KdV and Kawahara equations are solved using ARPSM and ATIM. These methods provide more precise numerical answers when compared with other numerical techniques. Additionally, a comparison analysis is performed on the numerical findings. The suggested approaches' findings are consistent with one another, which is a strong indicator of their efficacy and reliability. For various values of fractional-order derivatives, there is additional graphical importance. Therefore, the methods are accurate, easy to implement, not affected by computational error phases, and quick. This study lays the groundwork for researchers to quickly solve various PDEs.

2. Basics of fractional calculus

Definition 2.1. [37] Assume that $\eta(\epsilon, \Omega)$ is an exponential order continuous function. The definition of the Aboodh transform (AT), assuming $\sigma \geq 0$ for $\eta(\epsilon, \Omega)$, is as follows:

$$A[\eta(\epsilon, \Omega)] = \Psi(\epsilon, \xi) = \frac{1}{\xi} \int_0^\infty \eta(\epsilon, \Omega) e^{-\Omega\xi} d\Omega, \quad r_1 \leq \xi \leq r_2.$$

The Aboodh inverse transform (AIT) is given as:

$$A^{-1}[\Psi(\epsilon, \xi)] = \eta(\epsilon, \Omega) = \frac{1}{2\pi i} \int_{u-i\infty}^{u+i\infty} \Psi(\epsilon, \Omega) \xi e^{\Omega\xi} d\Omega,$$

where $\epsilon = (\epsilon_1, \epsilon_2, \cdots, \epsilon_p) \in \mathbb{R}^p$ and $p \in \mathbb{N}$.

Lemma 2.1. *[38, 39] It is assumed that there exist two exponentially ordered, piecewise continuous functions $\eta_1(\epsilon, \Omega)$ and $\eta_2(\epsilon, \Omega)$ on $[0, \infty]$. Let $A[\eta_1(\epsilon, \Omega)] = \Psi_1(\epsilon, \Omega), A[\eta_2(\epsilon, \Omega)] = \Psi_2(\epsilon, \Omega)$, and χ_1, χ_2 be arbitrary constants. These characteristics are thus true:*

(1) $A[\chi_1\eta_1(\epsilon,\Omega)+\chi_2\eta_2(\epsilon,\Omega)]=\chi_1\Psi_1(\epsilon,\xi)+\chi_2\Psi_2(\epsilon,\Omega)$,

(2) $A^{-1}[\chi_1\Psi_1(\epsilon,\Omega)+\chi_2\Psi_2(\epsilon,\Omega)]=\chi_1\eta_1(\epsilon,\xi)+\chi_2\eta_2(\epsilon,\Omega)$,

(3) $A[J^p_\Omega\eta(\epsilon,\Omega)]=\frac{\Psi(\epsilon,\xi)}{\xi^p}$,

(4) $A[D^p_\Omega\eta(\epsilon,\Omega)]=\xi^p\Psi(\epsilon,\xi)-\sum_{K=0}^{r-1}\frac{\eta^K(\epsilon,0)}{\xi^{K-p+2}}, r-1<p\le r,\ r\in\mathbb{N}.$

Definition 2.2. [40] In terms of order p, the function $\eta(\epsilon,\Omega)$ has derivative of fractional order as stated by Caputo.

$$D^p_\Omega\eta(\epsilon,\Omega)=J^{m-p}_\Omega\eta^{(m)}(\epsilon,\Omega),\ m-1<p\le m,\ r\ge 0,$$

where $\epsilon=(\epsilon_1,\epsilon_2,\cdots,\epsilon_p)\in\mathbb{R}^p$ and $p,m\in R$, J^{m-p}_Ω is the integral of the Riemann-Liouville of $\eta(\epsilon,\Omega)$.

Definition 2.3. [41] The representation of power series is composed of the following structure.

$$\sum_{r=0}^{\infty}\hbar_r(\epsilon)(\Omega-\Omega_0)^{rp}=1+\hbar_1(\Omega-\Omega_0)^p+\hbar_2(\Omega-\Omega_0)^{2p}+\cdots,$$

where $\epsilon=(\epsilon_1,\epsilon_2,\cdots,\epsilon_p)\in\mathbb{R}^p$ and $p\in\mathbb{N}$. This is known as the multiple fractional power series concerning Ω_0, where Ω and $\hbar_r(\epsilon)'s$ are variable and series coefficients, respectively.

Lemma 2.2. *Consider the exponential order function is denoted as* $\eta(\epsilon,\Omega)$. $A[\eta(\epsilon,\Omega)]=\Psi(\epsilon,\xi)$ *is the description of the AT in this case. Hence,*

$$A[D^{rp}_\Omega\eta(\epsilon,\Omega)]=\xi^{rp}\Psi(\epsilon,\xi)-\sum_{j=0}^{r-1}\xi^{p(r-j)-2}D^{jp}_\Omega\eta(\epsilon,0), 0<p\le 1, \tag{2.1}$$

where $\epsilon=(\epsilon_1,\epsilon_2,\cdots,\epsilon_p)\in\mathbb{R}^p$ and $p\in\mathbb{N}$ and $D^{rp}_\Omega=D^p_\Omega.D^p_\Omega.\cdots.D^p_\Omega(r-times)$

Proof. By using the induction method, we have to prove Eq (2.1). In Eq (2.1), substitute $r=1$.

$$A[D^p_\Omega\eta(\epsilon,\Omega)]=\xi^p\Psi(\epsilon,\xi)-\xi^{p-2}\eta(\epsilon,0)-\xi^{p-2}D^p_\Omega\eta(\epsilon,0).$$

On the bases of Lemma 2.1, Eq (2.1) for $r=1$ holds true. Put $r=2$ in Eq (2.1).

$$A[D^{2p}_r\eta(\epsilon,\Omega)]=\xi^{2p}\Psi(\epsilon,\xi)-\xi^{2p-2}\eta(\epsilon,0)-\xi^{p-2}D^p_\Omega\eta(\epsilon,0). \tag{2.2}$$

From left-hand side (LHS) of Eq (2.2), we obtain:

$$LHS=A[D^{2p}_\Omega\eta(\epsilon,\Omega)]. \tag{2.3}$$

The expressions for Eq (2.3) are as follows:

$$LHS=A[D^p_\Omega\eta(\epsilon,\Omega)]. \tag{2.4}$$

Assume

$$z(\epsilon,\Omega)=D^p_\Omega\eta(\epsilon,\Omega). \tag{2.5}$$

This makes Eq (2.4) as

$$LHS = A[D_{\Omega}^{p} z(\epsilon, \Omega)]. \tag{2.6}$$

From the definition of the derivative of Caputo, we make changes in Eq (2.6).

$$LHS = A[J^{1-p} z^{'}(\epsilon, \Omega)]. \tag{2.7}$$

By applying the Riemann-Liouville integral Eq (2.7), we obtain:

$$LHS = \frac{A[z^{'}(\epsilon, \Omega)]}{\xi^{1-p}}. \tag{2.8}$$

By using the AT feature of differentiability, Eq (2.8) is modified:

$$LHS = \xi^{p} Z(\epsilon, \xi) - \frac{z(\epsilon, 0)}{\xi^{2-p}}. \tag{2.9}$$

From Eq (2.5), we derive:

$$Z(\epsilon, \xi) = \xi^{p} \Psi(\epsilon, \xi) - \frac{\eta(\epsilon, 0)}{\xi^{2-p}},$$

where $A[z(\epsilon, \Omega)] = Z(\epsilon, \xi)$. Hence, Eq (2.9) becomes

$$LHS = \xi^{2p} \Psi(\epsilon, \xi) - \frac{\eta(\epsilon, 0)}{\xi^{2-2p}} - \frac{D_{\Omega}^{p} \eta(\epsilon, 0)}{\xi^{2-p}}. \tag{2.10}$$

Let's suppose Eq (2.1) holds true for $r = K$. Substitute $r = K$ in Eq (2.1):

$$A[D_{\Omega}^{Kp} \eta(\epsilon, \Omega)] = \xi^{Kp} \Psi(\epsilon, \xi) - \sum_{j=0}^{K-1} \xi^{p(K-j)-2} D_{\Omega}^{jp} D_{\Omega}^{jp} \eta(\epsilon, 0), \ 0 < p \leq 1. \tag{2.11}$$

Substituting $r = K + 1$ in Eq (2.1):

$$A[D_{\Omega}^{(K+1)p} \eta(\epsilon, \Omega)] = \xi^{(K+1)p} \Psi(\epsilon, \xi) - \sum_{j=0}^{K} \xi^{p((K+1)-j)-2} D_{\Omega}^{jp} \eta(\epsilon, 0). \tag{2.12}$$

After analyzing Eq (2.12)'s LHS, we deduce

$$LHS = A[D_{\Omega}^{Kp} (D_{\Omega}^{Kp})]. \tag{2.13}$$

Let

$$D_{\Omega}^{Kp} = g(\epsilon, \Omega).$$

By Eq (2.13), we drive

$$LHS = A[D_{\Omega}^{p} g(\epsilon, \Omega)]. \tag{2.14}$$

By using the integral of the Riemann-Liouville and derivative of Caputo on Eq (2.14), the subsequent result can be obtained.

$$LHS = \xi^{p} A[D_{\Omega}^{Kp} \eta(\epsilon, \Omega)] - \frac{g(\epsilon, 0)}{\xi^{2-p}}. \tag{2.15}$$

To get Eq (2.15), use Eq (2.11).

$$LHS = \xi^{rp}\Psi(\epsilon,\xi) - \sum_{j=0}^{r-1} \xi^{p(r-j)-2} D_{\Omega}^{jp}\eta(\epsilon,0). \tag{2.16}$$

In addition, Eq (2.16) produces the subsequent outcome.

$$LHS = A[D_{\Omega}^{rp}\eta(\epsilon,0)].$$

Thus, for $r = K+1$, Eq (2.1) holds. For all positive integers, Eq (2.1) holds true according to the mathematical induction technique. □

A deeper understanding of the ARPSM and multiple fractional Taylor series (MFTS) are given as follow.

Lemma 2.3. *Consider the function $\eta(\epsilon,\Omega)$ is an exponential order. $A[\eta(\epsilon,\Omega)] = \Psi(\epsilon,\xi)$ is the expression that signifies the AT of $\eta(\epsilon,\Omega)$. AT is represented as follows in MFTS notation:*

$$\Psi(\epsilon,\xi) = \sum_{r=0}^{\infty} \frac{\hbar_r(\epsilon)}{\xi^{rp+2}}, \xi > 0, \tag{2.17}$$

where, $\epsilon = (s_1, \epsilon_2, \cdots, \epsilon_p) \in \mathbb{R}^p,\ p \in \mathbb{N}$.

Proof. Consider the Taylor's series:

$$\eta(\epsilon,\Omega) = \hbar_0(\epsilon) + \hbar_1(\epsilon)\frac{\Omega^p}{\Gamma[p+1]}AA + \hbar_2(\epsilon)\frac{\Omega^{2p}}{\Gamma[2p+1]} + \cdots. \tag{2.18}$$

The subsequent equality is produced when the AT is applied to Eq (2.18):

$$A\left[\eta(\epsilon,\Omega)\right] = A\left[\hbar_0(\epsilon)\right] + A\left[\hbar_1(\epsilon)\frac{\Omega^p}{\Gamma[p+1]}\right] + A\left[\hbar_1(\epsilon)\frac{\Omega^{2p}}{\Gamma[2p+1]}\right] + \cdots.$$

This is achieved by utilizing the AT's features.

$$A\left[\eta(\epsilon,\Omega)\right] = \hbar_0(\epsilon)\frac{1}{\xi^2} + \hbar_1(\epsilon)\frac{1}{\Gamma[p+1]}\frac{1}{\xi^{p+2}} + \hbar_2(\epsilon)\frac{1}{\Gamma[2p+1]}\frac{1}{\xi^{2p+2}}\cdots.$$

Hence, by Eq (2.17), a new Taylor's series is obtained: □

Lemma 2.4. *Let the multiple fractional power series (MFPS) be expressed in terms of Taylor's series new form Eq (2.17), $A[\eta(\epsilon,\Omega)] = \Psi(\epsilon,\xi)$.*

$$\hbar_0(\epsilon) = \lim_{\xi\to\infty} \xi^2\Psi(\epsilon,\xi) = \eta(\epsilon,0). \tag{2.19}$$

Proof. Let's suppose the Taylor's series:

$$\hbar_0(\epsilon) = \xi^2\Psi(\epsilon,\xi) - \frac{\hbar_1(\epsilon)}{\xi^p} - \frac{\hbar_2(\epsilon)}{\xi^{2p}} - \cdots. \tag{2.20}$$

As denoted by Eq (2.20), the necessary solution can be obtained by employing $lim_{x\to\infty}$ in Eq (2.19) and performing a short calculation. □

Theorem 2.5. *The following is an MFPS representation of the function* $A[\eta(\epsilon,\Omega)] = \Psi(\epsilon,\xi)$*:*

$$\Psi(\epsilon,\xi) = \sum_{0}^{\infty} \frac{\hbar_r(\epsilon)}{\xi^{rp+2}},\ \xi > 0,$$

where $\epsilon = (\epsilon_1, \epsilon_2, \cdots, \epsilon_p) \in \mathbb{R}^p$ *and* $p \in \mathbb{N}$*. Then, we have*

$$\hbar_r(\epsilon) = D_r^{rp}\eta(\epsilon, 0),$$

where, $D_\Omega^{rp} = D_\Omega^p.D_\Omega^p.\cdots.D_\Omega^p(r - times)$*.*

Proof. Let's suppose the Taylor's series:

$$\hbar_1(\epsilon) = \xi^{p+2}\Psi(\epsilon,\xi) - \xi^p\hbar_0(\epsilon) - \frac{\hbar_2(\epsilon)}{\xi^p} - \frac{\hbar_3(\epsilon)}{\xi^{2p}} - \cdots \tag{2.21}$$

$\lim_{\xi\to\infty}$, is applied to Eq (2.21), and we get

$$\hbar_1(\epsilon) = \lim_{\xi\to\infty}(\xi^{p+2}\Psi(\epsilon,\xi) - \xi^p\hbar_0(\epsilon)) - \lim_{\xi\to\infty}\frac{\hbar_2(\epsilon)}{\xi^p} - \lim_{\xi\to\infty}\frac{\hbar_3(\epsilon)}{\xi^{2p}} - \cdots.$$

The equality that results from taking the limit is as follows:

$$\hbar_1(\epsilon) = \lim_{\xi\to\infty}(\xi^{p+2}\Psi(\epsilon,\xi) - \xi^p\hbar_0(\epsilon)). \tag{2.22}$$

Using Lemma 2.2, we obtain:

$$\hbar_1(\epsilon) = \lim_{\xi\to\infty}(\xi^2 A[D_\Omega^p\eta(\epsilon,\Omega)](\xi)). \tag{2.23}$$

Furthermore, the Eq (2.23) is modified using Lemma 2.3.

$$\hbar_1(\epsilon) = D_\Omega^p\eta(\epsilon, 0).$$

Using Taylor's series and applying $limit_{\xi\to\infty}$ again, we obtain:

$$\hbar_2(\epsilon) = \xi^{2p+2}\Psi(\epsilon,\xi) - \xi^{2p}\hbar_0(\epsilon) - \xi^p\hbar_1(\epsilon) - \frac{\hbar_3(\epsilon)}{\xi^p} - \cdots.$$

Lemma 2.3 gives us the result

$$\hbar_2(\epsilon) = \lim_{\xi\to\infty}\xi^2(\xi^{2p}\Psi(\epsilon,\xi) - \xi^{2p-2}\hbar_0(\epsilon) - \xi^{p-2}\hbar_1(\epsilon)). \tag{2.24}$$

Equation (2.24) is transformed using Lemmas 2.2 and Eq (2.4).

$$\hbar_2(\epsilon) = D_\Omega^{2p}\eta(\epsilon, 0).$$

Apply the same procedure and Taylor series, and we obtain:

$$\hbar_3(\epsilon) = \lim_{\xi\to\infty}\xi^2(A[D_\Omega^{2p}\eta(\epsilon, p)](\xi)).$$

Finally, we get:

$$\hbar_3(\epsilon) = D_\Omega^{3p}\eta(\epsilon, 0).$$

In general,

$$\hbar_r(\epsilon) = D_\Omega^{rp}\eta(\epsilon, 0),$$

is proved. □

The new Taylor series has the conditions for the convergence given in the subsequent theorem.

Theorem 2.6. *The expression for MFTS is given in Lemma 2.3 and can be expressed as:* $A[\eta(\epsilon,\Omega)] = \Psi(\epsilon,\xi)$. *When* $|\xi^a A[D_\Omega^{(K+1)p}\eta(\epsilon,\Omega)]| \leq T$, $\forall\ 0 < p \leq 1$, *and* $0 < \xi \leq s$, $R_K(\epsilon,\xi)$ *is the residual of the new MFTS satisfying:*

$$|R_K(\epsilon,\xi)| \leq \frac{T}{\xi^{(K=1)p+2}},\ 0 < \xi \leq s.$$

Proof. For $r = 0, 1, 2, \cdots, K+1$, and $0 < \xi \leq s$, we consider to define $A[D_\Omega^{rp}\eta(\epsilon,\Omega)](\xi)$. Utilize the Taylor series to derive the subsequent relation:

$$R_K(\epsilon,\xi) = \Psi(\epsilon,\xi) - \sum_{r=0}^{K} \frac{\hbar_r(\epsilon)}{\xi^{rp+2}}. \tag{2.25}$$

Apply Theorem 2.5 on Eq (2.25) to obtain:

$$R_K(\epsilon,\xi) = \Psi(\epsilon,\xi) - \sum_{r=0}^{K} \frac{D_\Omega^{rp}\eta(\epsilon,0)}{\xi^{rp+2}}. \tag{2.26}$$

$\xi^{(K+1)a+2}$ is to be multiplied with Eq (2.26) to obtain the following form.

$$\xi^{p(K+1)+2}R_K(\epsilon,\xi) = \xi^2(\xi^{p(K+1)}\Psi(\epsilon,\xi) - \sum_{r=0}^{K} \xi^{p(K+1-r)-2}D_\Omega^{rp}\eta(\epsilon,0)). \tag{2.27}$$

Equation (2.27) is modified with Lemma 2.2:

$$\xi^{p(K+1)+2}R_K(\epsilon,\xi) = \xi^2 A[D_\Omega^{p(K+1)}\eta(\epsilon,\Omega)]. \tag{2.28}$$

The absolute of Eq (2.28) gives us

$$|\xi^{p(K+1)+2}R_K(\epsilon,\xi)| = |\xi^2 A[D_\Omega^{p(K+1)}\eta(\epsilon,\Omega)]|. \tag{2.29}$$

By applying the conditions listed in Eq (2.29), the subsequent result is achieved.

$$\frac{-T}{\xi^{p(K+1)+2}} \leq R_K(\epsilon,\xi) \leq \frac{T}{\xi^{p(K+1)+2}}. \tag{2.30}$$

Equation (2.30) yields the desired outcome.

$$|R_K(\epsilon,\xi)| \leq \frac{T}{\xi^{p(K+1)+2}}.$$

Therefore, new conditions for the series to converge are developed. □

3. Methodologies

3.1. ARPSM technique

In this paper, we explain how ARPSM rules formed the basis of our solution.
Step 1: Assume the general PDE:

$$D_{\Omega}^{qp}\eta(\epsilon,\Omega) + \vartheta(\epsilon)N(\eta) - \delta(\epsilon,\eta) = 0. \tag{3.1}$$

Step 2: Apply the AT on Eq (3.1):

$$A[D_{\Omega}^{qp}\eta(\epsilon,\Omega) + \vartheta(\epsilon)N(\eta) - \delta(\epsilon,\eta)] = 0. \tag{3.2}$$

Utilizing Lemma 2.1 to modify Eq (3.2),

$$\Psi(\epsilon,s) = \sum_{j=0}^{q-1}\frac{D_{\Omega}^{j}\eta(\epsilon,0)}{s^{qp+2}} - \frac{\vartheta(\epsilon)Y(s)}{s^{qp}} + \frac{F(\epsilon,s)}{s^{qp}}, \tag{3.3}$$

where $A[\delta(\epsilon,\eta)] = F(\epsilon,s), A[N(\eta)] = Y(s)$.
Step 3: Equation (3.3) takes the following form:

$$\Psi(\epsilon,s) = \sum_{r=0}^{\infty}\frac{\hbar_r(\epsilon)}{s^{rp+2}},\ s>0.$$

Step 4: Take the steps listed below:

$$\hbar_0(\epsilon) = \lim_{s\to\infty} s^2\Psi(\epsilon,s) = \eta(\epsilon,0).$$

Use Theorem 2.6 to obtain this form.

$$\hbar_1(\epsilon) = D_{\Omega}^{p}\eta(\epsilon,0),$$

$$\hbar_2(\epsilon) = D_{\Omega}^{2p}\eta(\epsilon,0),$$

$$\vdots$$

$$\hbar_w(\epsilon) = D_{\Omega}^{wp}\eta(\epsilon,0).$$

Step 5: The K^{th} truncated series $\Psi(\epsilon,s)$ can be obtained using the following expression:

$$\Psi_K(\epsilon,s) = \sum_{r=0}^{K}\frac{\hbar_r(\epsilon)}{s^{rp+2}},\ s>0,$$

$$\Psi_K(\epsilon,s) = \frac{\hbar_0(\epsilon)}{s^2} + \frac{\hbar_1(\epsilon)}{s^{p+2}} + \cdots + \frac{\hbar_w(\epsilon)}{s^{wp+2}} + \sum_{r=w+1}^{K}\frac{\hbar_r(\epsilon)}{s^{rp+2}}.$$

Step 6: Note that the residual Aboodh function (RAF) (3.3) and the K^{th}-truncated RAF must be considered independently to obtain:

$$ARes(\epsilon, s) = \Psi(\epsilon, s) - \sum_{j=0}^{q-1} \frac{D_{\Omega}^{j}\eta(\epsilon, 0)}{s^{jp+2}} + \frac{\vartheta(\epsilon)Y(s)}{s^{jp}} - \frac{F(\epsilon, s)}{s^{jp}},$$

and

$$ARes_K(\epsilon, s) = \Psi_K(\epsilon, s) - \sum_{j=0}^{q-1} \frac{D_{\Omega}^{j}\eta(\epsilon, 0)}{s^{jp+2}} + \frac{\vartheta(\epsilon)Y(s)}{s^{jp}} - \frac{F(\epsilon, s)}{s^{jp}}. \tag{3.4}$$

Step 7: Equation (3.4) may be substituted with $\Psi_K(\epsilon, s)$ in place of its expansion form.

$$\begin{aligned} ARes_K(\epsilon, s) &= \Big(\frac{\hbar_0(\epsilon)}{s^2} + \frac{\hbar_1(\epsilon)}{s^{p+2}} + \cdots + \frac{\hbar_w(\epsilon)}{s^{wp+2}} + \sum_{r=w+1}^{K} \frac{\hbar_r(\epsilon)}{s^{rp+2}}\Big) \\ &- \sum_{j=0}^{q-1} \frac{D_{\Omega}^{j}\eta(\epsilon, 0)}{s^{jp+2}} + \frac{\vartheta(\epsilon)Y(s)}{s^{jp}} - \frac{F(\epsilon, s)}{s^{jp}}. \end{aligned} \tag{3.5}$$

Step 8: Multifly s^{Kp+2} on either side of the equation to get the solution to Eq (3.5).

$$\begin{aligned} s^{Kp+2}ARes_K(\epsilon, s) &= s^{Kp+2}\Big(\frac{\hbar_0(\epsilon)}{s^2} + \frac{\hbar_1(\epsilon)}{s^{p+2}} + \cdots + \frac{\hbar_w(\epsilon)}{s^{wp+2}} + \sum_{r=w+1}^{K} \frac{\hbar_r(\epsilon)}{s^{rp+2}} \\ &- \sum_{j=0}^{q-1} \frac{D_{\Omega}^{j}\eta(\epsilon, 0)}{s^{jp+2}} + \frac{\vartheta(\epsilon)Y(s)}{s^{jp}} - \frac{F(\epsilon, s)}{s^{jp}}\Big). \end{aligned} \tag{3.6}$$

Step 9: Take $\lim_{s\to\infty}$ of Eq (3.6) to obtain:

$$\begin{aligned} \lim_{s\to\infty} s^{Kp+2}ARes_K(\epsilon, s) &= \lim_{s\to\infty} s^{Kp+2}\Big(\frac{\hbar_0(\epsilon)}{s^2} + \frac{\hbar_1(\epsilon)}{s^{p+2}} + \cdots + \frac{\hbar_w(\epsilon)}{s^{wp+2}} + \sum_{r=w+1}^{K} \frac{\hbar_r(\epsilon)}{s^{rp+2}} \\ &- \sum_{j=0}^{q-1} \frac{D_{\Omega}^{j}\eta(\epsilon, 0)}{s^{jp+2}} + \frac{\vartheta(\epsilon)Y(s)}{s^{jp}} - \frac{F(\epsilon, s)}{s^{jp}}\Big). \end{aligned}$$

Step 10: $\hbar_K(\epsilon)$ values can be obtained using the equation above.

$$\lim_{s\to\infty}(s^{Kp+2}ARes_K(\epsilon, s)) = 0,$$

where $K = 1 + w, 2 + w, \cdots$.
Step 11: Values of $\hbar_K(\epsilon)$ are then substituted in Eq (3.3).
Step 12: Taking the inverse AT we obtain the final solution $\eta_K(\epsilon, \Omega)$.

3.2. ATIM Technique

Let's consider the PDE as given below:

$$D_{\Omega}^{p}\eta(\epsilon, \Omega) = \Phi\Big(\eta(\epsilon, \Omega), D_{\epsilon}^{\Omega}\eta(\epsilon, \Omega), D_{\epsilon}^{2\Omega}\eta(\epsilon, \Omega), D_{\epsilon}^{3\Omega}\eta(\epsilon, \Omega)\Big),\ 0 < p, \Omega \leq 1. \tag{3.7}$$

The initial condition is

$$\eta^{(\hbar)}(\epsilon,0)=h_{\hbar},\ \hbar=0,1,2,\cdots,m-1. \tag{3.8}$$

The function to be determined is $\eta(\epsilon,\Omega)$, while $\Phi\Big(\eta(\epsilon,\Omega),D_{\epsilon}^{\Omega}\eta(\epsilon,\Omega),D_{\epsilon}^{2\Omega}\eta(\epsilon,\Omega)D_{\epsilon}^{3\Omega}\eta(\epsilon,\Omega)\Big)$ are operators of $\eta(\epsilon,\Omega),D_{\epsilon}^{\Omega}\eta(\epsilon,\Omega),D_{\epsilon}^{2\Omega}\eta(\epsilon,\Omega)$ and $D_{\epsilon}^{3\Omega}\eta(\epsilon,\Omega)$. The AT is applied on Eq (3.7) to obtain:

$$A[\eta(\epsilon,\Omega)]=\frac{1}{s^{p}}\Big(\sum_{\hbar=0}^{m-1}\frac{\eta^{(\hbar)}(\epsilon,0)}{s^{2-p+\hbar}}+A\Big[\Phi\Big(\eta(\epsilon,\Omega),D_{\epsilon}^{\Omega}\eta(\epsilon,\Omega),D_{\epsilon}^{2\Omega}\eta(\epsilon,\Omega),D_{\epsilon}^{3\Omega}\eta(\epsilon,\Omega)\Big)\Big]\Big). \tag{3.9}$$

The AIT yields the solution to this problem:

$$\eta(\epsilon,\Omega)=A^{-1}\Big[\frac{1}{s^{p}}\Big(\sum_{\hbar=0}^{m-1}\frac{\eta^{(\hbar)}(\epsilon,0)}{s^{2-p+\hbar}}+A\Big[\Phi\Big(\eta(\epsilon,\Omega),D_{\epsilon}^{\Omega}\eta(\epsilon,\Omega),D_{\epsilon}^{2\Omega}\eta(\epsilon,\Omega),D_{\epsilon}^{3\Omega}\eta(\epsilon,\Omega)\Big)\Big]\Big)\Big]. \tag{3.10}$$

An infinite series denotes the ATIM-derived solution.

$$\eta(\epsilon,\Omega)=\sum_{i=0}^{\infty}\eta_{i}. \tag{3.11}$$

$\Phi\Big(\eta,D_{\epsilon}^{\Omega}\eta,D_{\epsilon}^{2\Omega}\eta,D_{\epsilon}^{3\Omega}\eta\Big)$ can be decomposed as:

$$\begin{aligned}\Phi\Big(\eta,D_{\epsilon}^{\Omega}\eta,D_{\epsilon}^{2\Omega}\eta,D_{\epsilon}^{3\Omega}\eta\Big)&=\Phi\Big(\eta_{0},D_{\epsilon}^{\Omega}\eta_{0},D_{\epsilon}^{2\Omega}\eta_{0},D_{\epsilon}^{3\Omega}\eta_{0}\Big)\\&+\sum_{i=0}^{\infty}\left(\Phi\Big(\sum_{\hbar=0}^{i}\Big(\eta_{\hbar},D_{\epsilon}^{\Omega}\eta_{\hbar},D_{\epsilon}^{2\Omega}\eta_{\hbar},D_{\epsilon}^{3\Omega}\eta_{\hbar}\Big)\Big)-\Phi\Big(\sum_{\hbar=1}^{i-1}\Big(\eta_{\hbar},D_{\epsilon}^{\Omega}\eta_{\hbar},D_{\epsilon}^{2\Omega}\eta_{\hbar},D_{\epsilon}^{3\Omega}\eta_{\hbar}\Big)\Big)\right).\end{aligned} \tag{3.12}$$

The subsequent equation is obtained by substituting the values of Eqs (3.11) and (3.12) for the initial equation (3.10).

$$\begin{aligned}\sum_{i=0}^{\infty}\eta_{i}(\epsilon,\Omega)&=A^{-1}\Big[\frac{1}{s^{p}}\Big(\sum_{\hbar=0}^{m-1}\frac{\eta^{(\hbar)}(\epsilon,0)}{s^{2-p+\hbar}}+A[\Phi(\eta_{0},D_{\epsilon}^{\Omega}\eta_{0},D_{\epsilon}^{2\Omega}\eta_{0},D_{\epsilon}^{3\Omega}\eta_{0})]\Big)\Big]\\&+A^{-1}\Big[\frac{1}{s^{p}}\Big(A\Big[\sum_{i=0}^{\infty}\Big(\Phi\sum_{\hbar=0}^{i}(\eta_{\hbar},D_{\epsilon}^{\Omega}\eta_{\hbar},D_{\epsilon}^{2\Omega}\eta_{\hbar},D_{\epsilon}^{3\Omega}\eta_{\hbar})\Big)\Big]\Big)\Big]\\&-A^{-1}\Big[\frac{1}{s^{p}}\Big(A\Big[\Big(\Phi\sum_{\hbar=1}^{i-1}(\eta_{\hbar},D_{\epsilon}^{\Omega}\eta_{\hbar},D_{\epsilon}^{2\Omega}\eta_{\hbar},D_{\epsilon}^{3\Omega}\eta_{\hbar})\Big)\Big]\Big)\Big]\end{aligned} \tag{3.13}$$

$$\begin{aligned}\eta_{0}(\epsilon,\Omega)&=A^{-1}\Big[\frac{1}{s^{p}}\Big(\sum_{\hbar=0}^{m-1}\frac{\eta^{(\hbar)}(\epsilon,0)}{s^{2-p+\hbar}}\Big)\Big],\\\eta_{1}(\epsilon,\Omega)&=A^{-1}\Big[\frac{1}{s^{p}}\Big(A[\Phi(\eta_{0},D_{\epsilon}^{\Omega}\eta_{0},D_{\epsilon}^{2\Omega}\eta_{0},D_{\epsilon}^{3\Omega}\eta_{0})]\Big)\Big],\\&\vdots\\\eta_{m+1}(\epsilon,\Omega)&=A^{-1}\Big[\frac{1}{s^{p}}\Big(A\Big[\sum_{i=0}^{\infty}\Big(\Phi\sum_{\hbar=0}^{i}(\eta_{\hbar},D_{\epsilon}^{\Omega}\eta_{\hbar},D_{\epsilon}^{2\Omega}\eta_{\hbar},D_{\epsilon}^{3\Omega}\eta_{\hbar})\Big)\Big]\Big)\Big]\\&-A^{-1}\Big[\frac{1}{s^{p}}\Big(A\Big[\Big(\Phi\sum_{\hbar=1}^{i-1}(\eta_{\hbar},D_{\epsilon}^{\Omega}\eta_{\hbar},D_{\epsilon}^{2\Omega}\eta_{\hbar},D_{\epsilon}^{3\Omega}\eta_{\hbar})\Big)\Big]\Big)\Big],\ m=1,2,\cdots.\end{aligned} \tag{3.14}$$

For the m-term of Eq (3.7), the analytically approximate solution may be obtained using the following expression:

$$\eta(\epsilon,\Omega)=\sum_{i=0}^{m-1}\eta_i. \tag{3.15}$$

4. Application of ARPSM and ATIM

4.1. Example 1 using ARPSM

Consider Kawahara equation of fractional order as follows:

$$D_{\Omega}^{p}\eta(\epsilon,\Omega)-\frac{\partial^5\eta(\epsilon,\Omega)}{\partial\epsilon^5}+\eta(\epsilon,\Omega)\frac{\partial^3\eta(\epsilon,\Omega)}{\partial\epsilon^3}+\eta(\epsilon,\Omega)\frac{\partial\eta(\epsilon,\Omega)}{\partial\epsilon}=0,\quad \text{where}\quad 0<p\leq 1, \tag{4.1}$$

with the initial condition:

$$\eta(\epsilon,0)=\frac{105}{169}\text{sech}^4\left(\frac{\epsilon-2}{2\sqrt{13}}\right), \tag{4.2}$$

and exact solution

$$\eta(\epsilon,\Omega)=\frac{105}{169}\text{sech}^4\left(\frac{-\frac{36\Omega}{169}+\epsilon-2}{2\sqrt{13}}\right).$$

Equation (4.2) is used, and AT is applied to Eq (4.1) to get

$$\begin{aligned}&\eta(\epsilon,s)-\frac{\frac{105}{169}\text{sech}^4\left(\frac{\epsilon-2}{2\sqrt{13}}\right)}{s^2}-\frac{1}{s^p}\Big[\frac{\partial^5\eta(\epsilon,s)}{\partial\epsilon^5}\Big]+\frac{1}{s^p}A_{\Omega}\Big[A_{\Omega}^{-1}\eta(\epsilon,s)\times\frac{\partial^3A_{\Omega}^{-1}\eta(\epsilon,s)}{\partial\epsilon^3}\Big]\\&+\frac{1}{s^p}A_{\Omega}\Big[A_{\Omega}^{-1}\eta(\epsilon,s)\times\frac{\partial A_{\Omega}^{-1}\eta(\epsilon,s)}{\partial\epsilon}\Big]=0.\end{aligned} \tag{4.3}$$

Therefore, the series k^{th}-truncated terms are:

$$\eta(\epsilon,s)=\frac{\frac{105}{169}\text{sech}^4\left(\frac{\epsilon-2}{2\sqrt{13}}\right)}{s^2}+\sum_{r=1}^{k}\frac{f_r(\epsilon,s)}{s^{rp+1}},\quad r=1,2,3,4\cdots. \tag{4.4}$$

Following is the RAF:

$$\begin{aligned}&A_{\Omega}Res(\epsilon,s)=\eta(\epsilon,s)-\frac{\frac{105}{169}\text{sech}^4\left(\frac{\epsilon-2}{2\sqrt{13}}\right)}{s^2}-\frac{1}{s^p}\Big[\frac{\partial^5\eta(\epsilon,s)}{\partial\epsilon^5}\Big]+\frac{1}{s^p}A_{\Omega}\Big[A_{\Omega}^{-1}\eta(\epsilon,s)\times\frac{\partial^3A_{\Omega}^{-1}\eta(\epsilon,s)}{\partial\epsilon^3}\Big]\\&+\frac{1}{s^p}A_{\Omega}\Big[A_{\Omega}^{-1}\eta(\epsilon,s)\times\frac{\partial A_{\Omega}^{-1}\eta(\epsilon,s)}{\partial\epsilon}\Big]=0,\end{aligned} \tag{4.5}$$

and the k^{th}-RAFs is:

$$\begin{aligned}&A_{\Omega}Res_k(\epsilon,s)=\eta_k(\epsilon,s)-\frac{\frac{105}{169}\text{sech}^4\left(\frac{\epsilon-2}{2\sqrt{13}}\right)}{s^2}-\frac{1}{s^p}\Big[\frac{\partial^5\eta_k(\epsilon,s)}{\partial\epsilon^5}\Big]+\frac{1}{s^p}A_{\Omega}\Big[A_{\Omega}^{-1}\eta_k(\epsilon,s)\times\frac{\partial^3A_{\Omega}^{-1}\eta_k(\epsilon,s)}{\partial\epsilon^3}\Big]\\&+\frac{1}{s^p}A_{\Omega}\Big[A_{\Omega}^{-1}\eta_k(\epsilon,s)\times\frac{\partial A_{\Omega}^{-1}\eta_k(\epsilon,s)}{\partial\epsilon}\Big]=0.\end{aligned} \tag{4.6}$$

It takes some calculation to find $f_r(\epsilon, s)$ for $r = 1, 2, 3, ...$ Using these procedures, we replace the r^{th}-truncated series Eq (4.4) for the r^{th}-RAF Eq (4.6), applying $\lim_{s\to\infty}(s^{rp+1})$ and solving $A_\Omega Res_{\eta,r}(\epsilon, s)) = 0$, for $r = 1, 2, 3, \cdots$. Some terms that we obtain are given below:

$$\begin{aligned} f_1(\epsilon, s) = &-\frac{105}{5940688\sqrt{13}}\Big(17290\sinh\Big(\frac{\epsilon-2}{2\sqrt{13}}\Big) - 10029\sinh\Big(\frac{3(\epsilon-2)}{2\sqrt{13}}\Big) - 2015\sinh\Big(\frac{5(\epsilon-2)}{2\sqrt{13}}\Big) \\ &+ 104\sinh\Big(\frac{7(\epsilon-2)}{2\sqrt{13}}\Big)\Big)\mathrm{sech}^{11}\Big(\frac{\epsilon-2}{2\sqrt{13}}\Big)\Big), \end{aligned} \tag{4.7}$$

$$\begin{aligned} f_2(\epsilon, s) = &\frac{105}{21718014715904}\Big(50957301372\cosh\Big(\frac{\epsilon-2}{\sqrt{13}}\Big) + 12586770193\cosh\Big(\frac{2(\epsilon-2)}{\sqrt{13}}\Big) \\ &- 12962735946\cosh\Big(\frac{3(\epsilon-2)}{\sqrt{13}}\Big) + 2020967026\cosh\Big(\frac{4(\epsilon-2)}{\sqrt{13}}\Big) + 68039374\cosh\Big(\frac{5(\epsilon-2)}{\sqrt{13}}\Big) \\ &- 9200529\cosh\Big(\frac{6(\epsilon-2)}{\sqrt{13}}\Big) + 43264\cosh\Big(\frac{7(\epsilon-2)}{\sqrt{13}}\Big) - 54264784626\Big)\mathrm{sech}^{18}\Big(\frac{\epsilon-2}{2\sqrt{13}}\Big), \end{aligned} \tag{4.8}$$

and so on.

For $r = 1, 2, 3, \cdots$, replace $f_r(\epsilon, s)$ in Eq (4.4):

$$\begin{aligned} \eta(\epsilon, s) = &\frac{\frac{105}{169}\mathrm{sech}^4\left(\frac{\epsilon-2}{2\sqrt{13}}\right)}{s^2} - \Big(\frac{105}{5940688\sqrt{13}}\Big(17290\sinh\Big(\frac{\epsilon-2}{2\sqrt{13}}\Big) - 10029\sinh\Big(\frac{3(\epsilon-2)}{2\sqrt{13}}\Big) \\ &- 2015\sinh\Big(\frac{5(\epsilon-2)}{2\sqrt{13}}\Big) + 104\sinh\Big(\frac{7(\epsilon-2)}{2\sqrt{13}}\Big)\Big)\mathrm{sech}^{11}\Big(\frac{\epsilon-2}{2\sqrt{13}}\Big)\Big)\Big)/\Big(s^{p+1}\Big) \\ &+ \Big(\frac{105}{21718014715904}\Big(50957301372\cosh\Big(\frac{\epsilon-2}{\sqrt{13}}\Big) + 12586770193\cosh\Big(\frac{2(\epsilon-2)}{\sqrt{13}}\Big) \\ &- 12962735946\cosh\Big(\frac{3(\epsilon-2)}{\sqrt{13}}\Big) + 2020967026\cosh\Big(\frac{4(\epsilon-2)}{\sqrt{13}}\Big) + 68039374\cosh\Big(\frac{5(\epsilon-2)}{\sqrt{13}}\Big) \\ &- 9200529\cosh\Big(\frac{6(\epsilon-2)}{\sqrt{13}}\Big) + 43264\cosh\Big(\frac{7(\epsilon-2)}{\sqrt{13}}\Big) - 54264784626\Big)\mathrm{sech}^{18}\Big(\frac{\epsilon-2}{2\sqrt{13}}\Big)\Big)\Big)/\Big(s^{2p+1}\Big) + \cdots. \end{aligned} \tag{4.9}$$

Apply AIT to obtain:

$$\begin{aligned} \eta(\epsilon, \Omega) = &\frac{105}{169}\mathrm{sech}^4\left(\frac{\epsilon-2}{2\sqrt{13}}\right) - \Omega^p\Big(\frac{105}{5940688\sqrt{13}}\Big(17290\sinh\Big(\frac{\epsilon-2}{2\sqrt{13}}\Big) - 10029\sinh\Big(\frac{3(\epsilon-2)}{2\sqrt{13}}\Big) \\ &- 2015\sinh\Big(\frac{5(\epsilon-2)}{2\sqrt{13}}\Big) + 104\sinh\Big(\frac{7(\epsilon-2)}{2\sqrt{13}}\Big)\Big)\mathrm{sech}^{11}\Big(\frac{\epsilon-2}{2\sqrt{13}}\Big)\Big)\Big)/\Big(\Gamma(p+1)\Big) \\ &+ \Omega^{2p}\Big(\frac{105}{21718014715904}\Big(50957301372\cosh\Big(\frac{\epsilon-2}{\sqrt{13}}\Big) + 12586770193\cosh\Big(\frac{2(\epsilon-2)}{\sqrt{13}}\Big) \\ &- 12962735946\cosh\Big(\frac{3(\epsilon-2)}{\sqrt{13}}\Big) + 2020967026\cosh\Big(\frac{4(\epsilon-2)}{\sqrt{13}}\Big) + 68039374\cosh\Big(\frac{5(\epsilon-2)}{\sqrt{13}}\Big) \\ &- 9200529\cosh\Big(\frac{6(\epsilon-2)}{\sqrt{13}}\Big) + 43264\cosh\Big(\frac{7(\epsilon-2)}{\sqrt{13}}\Big) - 54264784626\Big)\mathrm{sech}^{18}\Big(\frac{\epsilon-2}{2\sqrt{13}}\Big)\Big)\Big)/\Big(\Gamma(2p+1)\Big) + \cdots. \end{aligned} \tag{4.10}$$

Table 1 presents the ARPSM solution comparison for different values of the parameter p for $\Omega = 0.1$, illustrating how the choice of p impacts the accuracy and behavior of the solutions. Figure 1 shows a comparison between the approximate solution obtained using ARPSM (a) and the exact solution (b) for Example 1, confirming the high accuracy of the ARPSM approach. Figure 2 visualizes the impact of varying fractional orders on the ARPSM solution for different p values ($p = 0.32, 0.52, 0.72$), showcasing how changes in the fractional order influence the solution structure. Figure 3 extends the comparison in two dimensions, offering a 2D view of the fractional order solutions using ARPSM for the same values of p, further confirming the method's ability to capture the dynamics of fractional systems.

Table 1. ARPSM solution comparison for the values of p of Example 1 for $\Omega = 0.1$.

ϵ	$ARPSM_{p=0.52}$	$ARPSM_{p=0.72}$	$ARPSM_{p=1.00}$	$Exact$	$Error_{p=1.00}$
1.0	0.597480	0.597823	0.597918	0.597923	4.746940×10^{-6}
1.1	0.601882	0.602193	0.602280	0.602284	4.296239×10^{-6}
1.2	0.605857	0.606136	0.606214	0.606217	3.837431×10^{-6}
1.3	0.609395	0.609642	0.609710	0.609713	3.371748×10^{-6}
1.4	0.612487	0.612700	0.612759	0.612762	2.900316×10^{-6}
1.5	0.615125	0.615304	0.615354	0.615356	2.424166×10^{-6}
1.6	0.617301	0.617446	0.617486	0.617488	1.944232×10^{-6}
1.7	0.619010	0.619121	0.619151	0.619152	1.461368×10^{-6}
1.8	0.620248	0.620324	0.620344	0.620345	9.763596×10^{-7}
1.9	0.621010	0.621051	0.621061	0.621062	4.899361×10^{-7}
2.0	0.621296	0.621301	0.621302	0.621302	2.792130×10^{-8}

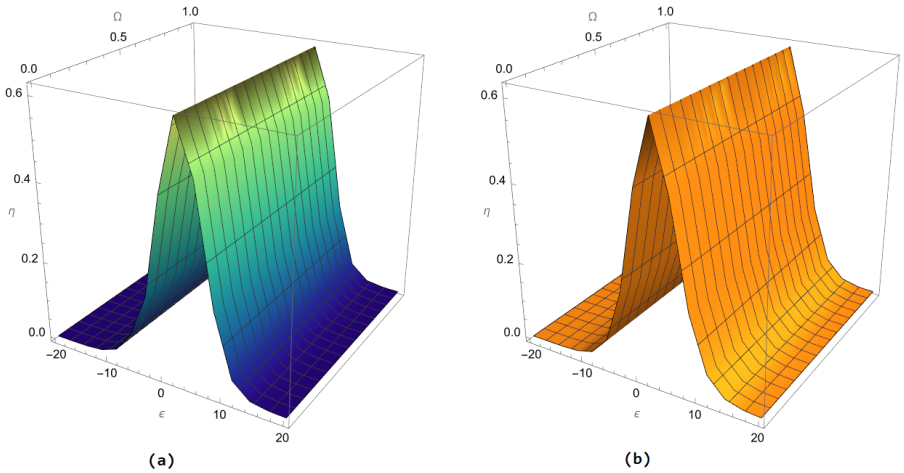

Figure 1. (a) ARPSM approximate solution, (b) exact solution.

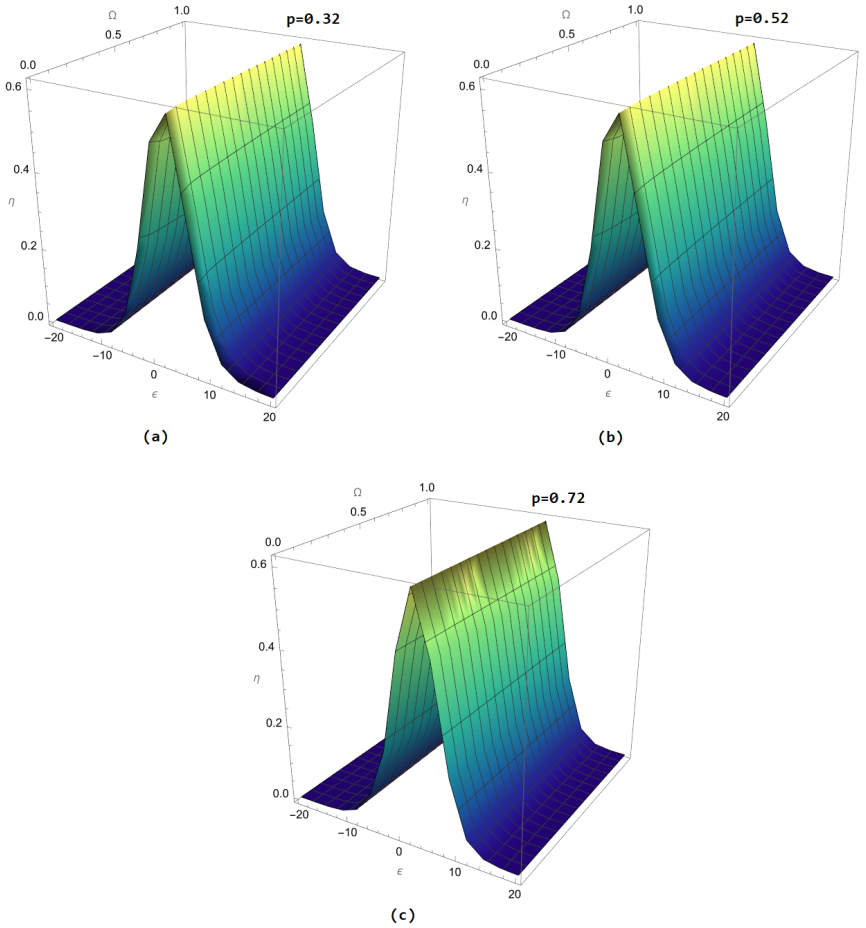

Figure 2. Fractional order comparison using ARPSM for $p = 0.32, 0.52, 0.72$.

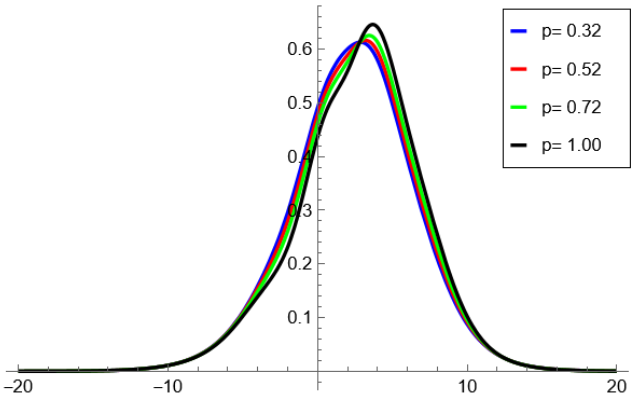

Figure 3. Fractional order 2D comparison using ARPSM for $p = 0.32, 0.52, 0.72$.

4.2. Example 1 using ATIM

Consider the Kawahara equation of fractional order:

$$D_{\Omega}^{p}\eta(\epsilon,\Omega) = \frac{\partial^5\eta(\epsilon,\Omega)}{\partial\epsilon^5} - \eta(\epsilon,\Omega)\frac{\partial^3\eta(\epsilon,\Omega)}{\partial\epsilon^3} - \eta(\epsilon,\Omega)\frac{\partial\eta(\epsilon,\Omega)}{\partial\epsilon}, \quad \text{where} \quad 0 < p \leq 1, \tag{4.11}$$

with the initial condition:

$$\eta(\epsilon,0)=\frac{105}{169}\text{sech}^4\left(\frac{\epsilon-2}{2\sqrt{13}}\right), \tag{4.12}$$

and exact solution

$$\eta(\epsilon,\Omega)=\frac{105}{169}\text{sech}^4\left(\frac{-\frac{36\Omega}{169}+\epsilon-2}{2\sqrt{13}}\right).$$

Apply AT on both sides of Eq (4.11) to obtain:

$$A[D_\Omega^p\eta(\epsilon,\Omega)]=\frac{1}{s^p}\Big(\sum_{k=0}^{m-1}\frac{\eta^{(k)}(\epsilon,0)}{s^{2-p+k}}+A\Big[\frac{\partial^5\eta(\epsilon,\Omega)}{\partial\epsilon^5}-\eta(\epsilon,\Omega)\frac{\partial^3\eta(\epsilon,\Omega)}{\partial\epsilon^3}-\eta(\epsilon,\Omega)\frac{\partial\eta(\epsilon,\Omega)}{\partial\epsilon}\Big]\Big). \tag{4.13}$$

Apply AIT on Eq (4.13) to obtain:

$$\eta(\epsilon,\Omega)=A^{-1}\Big[\frac{1}{s^p}\Big(\sum_{k=0}^{m-1}\frac{\eta^{(k)}(\epsilon,0)}{s^{2-p+k}}+A\Big[\frac{\partial^5\eta(\epsilon,\Omega)}{\partial\epsilon^5}-\eta(\epsilon,\Omega)\frac{\partial^3\eta(\epsilon,\Omega)}{\partial\epsilon^3}-\eta(\epsilon,\Omega)\frac{\partial\eta(\epsilon,\Omega)}{\partial\epsilon}\Big]\Big)\Big]. \tag{4.14}$$

Utilize AT iteratively to get:

$$\begin{aligned}\eta_0(\epsilon,\Omega)=&A^{-1}\Big[\frac{1}{s^p}\Big(\sum_{k=0}^{m-1}\frac{\eta^{(k)}(\epsilon,0)}{s^{2-p+k}}\Big)\Big]\\&=A^{-1}\Big[\frac{\eta(\epsilon,0)}{s^2}\Big]\\&=\frac{105}{169}\text{sech}^4\left(\frac{\epsilon-2}{2\sqrt{13}}\right).\end{aligned}$$

Applying the Riemann-Liouville integral on Eq (4.11),

$$\eta(\epsilon,\Omega)=\frac{105}{169}\text{sech}^4\left(\frac{\epsilon-2}{2\sqrt{13}}\right)-A\Big[\frac{\partial^5\eta(\epsilon,\Omega)}{\partial\epsilon^5}-\eta(\epsilon,\Omega)\frac{\partial^3\eta(\epsilon,\Omega)}{\partial\epsilon^3}-\eta(\epsilon,\Omega)\frac{\partial\eta(\epsilon,\Omega)}{\partial\epsilon}\Big]. \tag{4.15}$$

Using the ATIM technique, we provide the following terms:

$$\eta_0(\epsilon,\Omega)=\frac{105}{169}\text{sech}^4\left(\frac{\epsilon-2}{2\sqrt{13}}\right),$$

$$\eta_1(\epsilon,\Omega)=\frac{105}{2970344\sqrt{13}\Gamma(p+1)}\Omega^p\Big(11940\cosh\Big(\frac{\epsilon-2}{\sqrt{13}}\Big)+1911\cosh\Big(\frac{2(\epsilon-2)}{\sqrt{13}}\Big)-104\cosh\Big(\frac{3(\epsilon-2)}{\sqrt{13}}\Big)$$
$$-2675\Big)\tanh\Big(\frac{\epsilon-2}{2\sqrt{13}}\Big)\text{sech}^{10}\Big(\frac{\epsilon-2}{2\sqrt{13}}\Big),$$

$$\eta_2(\epsilon,\Omega)=\frac{105\Omega^{2p}\text{sech}^{18}\left(\frac{\epsilon-2}{2\sqrt{13}}\right)}{620288218300934144}\Big(\Big(35\sqrt{\frac{13}{\pi}}4^p\Omega^p\Gamma\Big(p+\frac{1}{2}\Big)\Big(13\Big(9385221\sinh\Big(\frac{1}{2}\sqrt{13}(\epsilon-2)\Big)$$
$$+120132725\sinh\Big(\frac{11(\epsilon-2)}{2\sqrt{13}}\Big)-910000\sinh\Big(\frac{15(\epsilon-2)}{2\sqrt{13}}\Big)+14144\sinh\Big(\frac{17(\epsilon-2)}{2\sqrt{13}}\Big)\Big)$$
$$+581521261600\sinh\Big(\frac{\epsilon-2}{2\sqrt{13}}\Big)-374464577051\sinh\Big(\frac{3(\epsilon-2)}{2\sqrt{13}}\Big)+130226023125\sinh\Big(\frac{5(\epsilon-2)}{2\sqrt{13}}\Big)$$

$$
\begin{aligned}
&-12004154204\sinh\Big(\frac{7(\epsilon-2)}{2\sqrt{13}}\Big)-7059672300\sinh\Big(\frac{9(\epsilon-2)}{2\sqrt{13}}\Big)\Big)\mathrm{sech}^7\Big(\frac{\epsilon-2}{2\sqrt{13}}\Big)\Big)/\Big(p^2\Gamma(p)\Gamma(3p)\Big)\\
&+\frac{28561}{\Gamma(2p+1)}\Big(50957301372\cosh\Big(\frac{\epsilon-2}{\sqrt{13}}\Big)+12586770193\cosh\Big(\frac{2(\epsilon-2)}{\sqrt{13}}\Big)\\
&-12962735946\cosh\Big(\frac{3(\epsilon-2)}{\sqrt{13}}\Big)+13\Big(155459002\cosh\Big(\frac{4(\epsilon-2)}{\sqrt{13}}\Big)+5233798\cosh\Big(\frac{5(\epsilon-2)}{\sqrt{13}}\Big)\\
&-707733\cosh\Big(\frac{6(\epsilon-2)}{\sqrt{13}}\Big)+3328\cosh\Big(\frac{7(\epsilon-2)}{\sqrt{13}}\Big)-4174214202\Big)\Big)\Big).
\end{aligned}
\tag{4.16}
$$

The final solution that is obtained via ATIM is given as:

$$
\eta(\epsilon,\Omega)=\eta_0(\epsilon,\Omega)+\eta_1(\epsilon,\Omega)+\eta_2(\epsilon,\Omega)+\cdots. \tag{4.17}
$$

$$
\begin{aligned}
\eta(\epsilon,\Omega)&=\frac{105}{169}\mathrm{sech}^4\left(\frac{\epsilon-2}{2\sqrt{13}}\right)+\frac{105}{2970344\sqrt{13}\Gamma(p+1)}\Omega^p\Big(11940\cosh\Big(\frac{\epsilon-2}{\sqrt{13}}\Big)\\
&+1911\cosh\Big(\frac{2(\epsilon-2)}{\sqrt{13}}\Big)-104\cosh\Big(\frac{3(\epsilon-2)}{\sqrt{13}}\Big)-2675\Big)\tanh\Big(\frac{\epsilon-2}{2\sqrt{13}}\Big)\mathrm{sech}^{10}\Big(\frac{\epsilon-2}{2\sqrt{13}}\Big)\\
&+\frac{105\Omega^{2p}\mathrm{sech}^{18}\Big(\frac{\epsilon-2}{2\sqrt{13}}\Big)}{620288218300934144}\Big(\Big(35\sqrt{\frac{13}{\pi}}4^p\Omega^p\Gamma\Big(p+\frac{1}{2}\Big)\Big(13\Big(9385221\sinh\Big(\frac{1}{2}\sqrt{13}(\epsilon-2)\Big)\\
&+120132725\sinh\Big(\frac{11(\epsilon-2)}{2\sqrt{13}}\Big)-910000\sinh\Big(\frac{15(\epsilon-2)}{2\sqrt{13}}\Big)+14144\sinh\Big(\frac{17(\epsilon-2)}{2\sqrt{13}}\Big)\Big)\\
&+581521261600\sinh\Big(\frac{\epsilon-2}{2\sqrt{13}}\Big)-374464577051\sinh\Big(\frac{3(\epsilon-2)}{2\sqrt{13}}\Big)+130226023125\sinh\Big(\frac{5(\epsilon-2)}{2\sqrt{13}}\Big)\\
&-12004154204\sinh\Big(\frac{7(\epsilon-2)}{2\sqrt{13}}\Big)-7059672300\sinh\Big(\frac{9(\epsilon-2)}{2\sqrt{13}}\Big)\Big)\mathrm{sech}^7\Big(\frac{\epsilon-2}{2\sqrt{13}}\Big)\Big)/\Big(p^2\Gamma(p)\Gamma(3p)\Big)\\
&+\frac{28561}{\Gamma(2p+1)}\Big(50957301372\cosh\Big(\frac{\epsilon-2}{\sqrt{13}}\Big)+12586770193\cosh\Big(\frac{2(\epsilon-2)}{\sqrt{13}}\Big)\\
&-12962735946\cosh\Big(\frac{3(\epsilon-2)}{\sqrt{13}}\Big)+13\Big(155459002\cosh\Big(\frac{4(\epsilon-2)}{\sqrt{13}}\Big)+5233798\cosh\Big(\frac{5(\epsilon-2)}{\sqrt{13}}\Big)\\
&-707733\cosh\Big(\frac{6(\epsilon-2)}{\sqrt{13}}\Big)+3328\cosh\Big(\frac{7(\epsilon-2)}{\sqrt{13}}\Big)-4174214202\Big)\Big)+\cdots.
\end{aligned}
\tag{4.18}
$$

Table 2 compares ATIM solutions for the same set of parameters, with similar trends observed as in ARPSM, demonstrating the robustness of both methods. Figure 4 juxtaposes the ATIM approximate solution (a) with the exact solution (b), verifying the precision of the ATIM method. Figure 5 compares the fractional order solutions using ATIM for ($p = 0.32, 0.52, 0.72$), and Figure 6 presents a 2D version of this comparison, highlighting the impact of the fractional order on the solution dynamics. Table 3 compares the absolute error for ARPSM and ATIM at $\Omega = 0.1$, demonstrating that both methods achieve highly accurate solutions with minimal error.

Table 2. ATIM solution comparison for the values of p of Example 1 for $\Omega = 0.1$.

ϵ	$ATIM_{p=0.52}$	$ATIM_{p=0.72}$	$ATIM_{p=1.00}$	$Exact$	$Error_{p=1.00}$
1.0	0.597546	0.597850	0.597917	0.597923	6.195481×10^{-6}
1.1	0.601942	0.602218	0.602278	0.602284	5.609848×10^{-6}
1.2	0.605911	0.606158	0.606212	0.606217	5.012997×10^{-6}
1.3	0.609443	0.609661	0.609709	0.609713	4.406507×10^{-6}
1.4	0.612528	0.612717	0.612758	0.612762	3.791852×10^{-6}
1.5	0.615160	0.615318	0.615353	0.615356	3.170410×10^{-6}
1.6	0.617329	0.617458	0.617485	0.617488	2.543461×10^{-6}
1.7	0.619032	0.619130	0.619150	0.619152	1.912204×10^{-6}
1.8	0.620263	0.620329	0.620343	0.620345	1.277767×10^{-6}
1.9	0.621019	0.621054	0.621061	0.621062	6.412226×10^{-7}
2.0	0.621298	0.621302	0.621302	0.621302	3.606186×10^{-8}

Table 3. The comparison of absolute error of Example 1 for $\Omega = 0.1$.

ϵ	$ARPSM_{p=1}$	$ATIM_{p=1}$	$Exact$	$Error_{ARPSM}$	$Error_{ATIM}$
1.0	0.597918	0.597917	0.597923	4.746940×10^{-6}	6.195481×10^{-6}
1.1	0.602280	0.602278	0.602284	4.296239×10^{-6}	5.609848×10^{-6}
1.2	0.606214	0.606212	0.606217	3.837431×10^{-6}	5.012997×10^{-6}
1.3	0.609710	0.609709	0.609713	3.371748×10^{-6}	4.406507×10^{-6}
1.4	0.612759	0.612758	0.612762	2.900316×10^{-6}	3.791852×10^{-6}
1.5	0.615354	0.615353	0.615356	2.424166×10^{-6}	3.170410×10^{-6}
1.6	0.617486	0.617485	0.617488	1.944232×10^{-6}	2.543461×10^{-6}
1.7	0.619151	0.619150	0.619152	1.461368×10^{-6}	1.912204×10^{-6}
1.8	0.620344	0.620343	0.620345	9.763596×10^{-7}	1.277767×10^{-6}
1.9	0.621061	0.621061	0.621062	4.899361×10^{-7}	6.412226×10^{-7}
2.0	0.621302	0.621302	0.621302	2.792130×10^{-8}	3.606186×10^{-8}

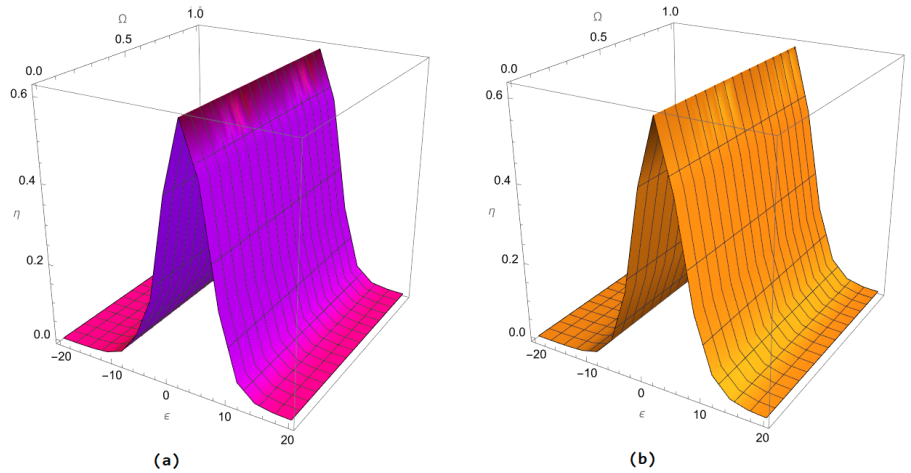

Figure 4. (a) ATIM approximate solution, (b) exact solution.

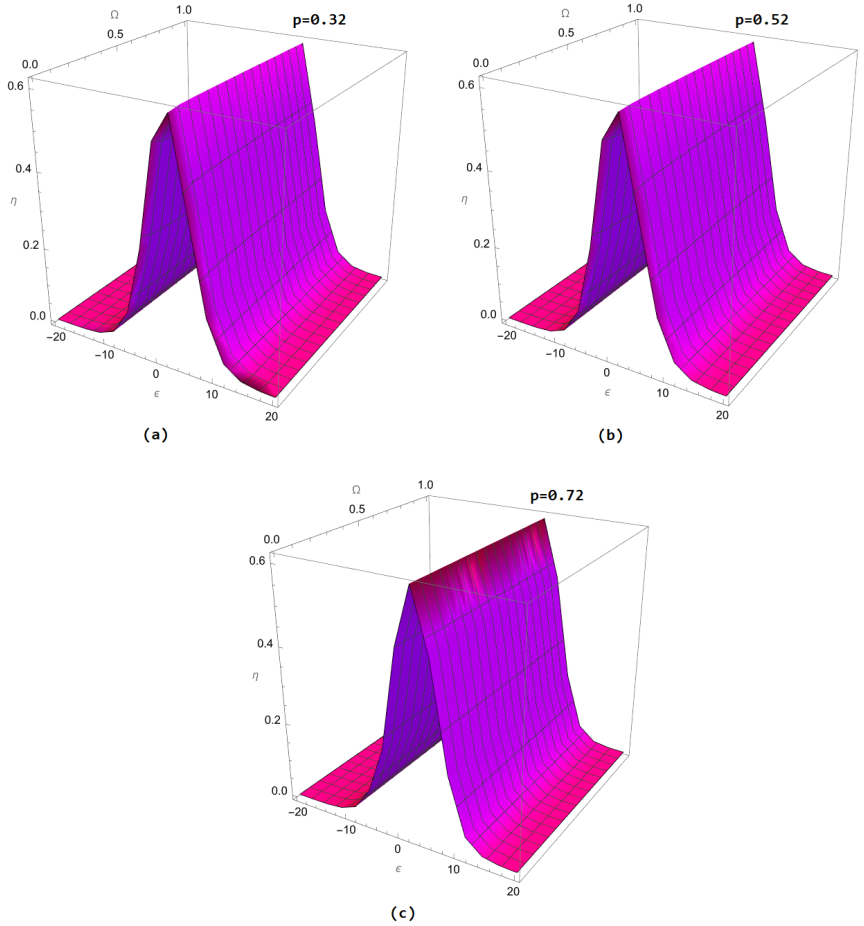

Figure 5. Fractional order comparison using ATIM for $p = 0.32, 0.52, 0.72$.

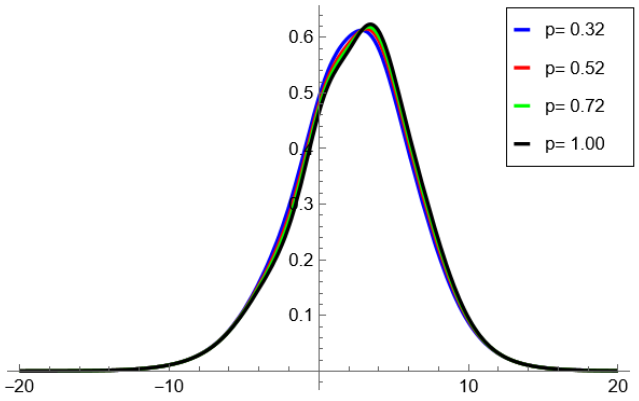

Figure 6. Fractional order 2D comparison using ATIM for $p = 0.32, 0.52, 0.72$.

4.3. Example 2 using ARPSM

Examine the famous fifth-order KdV equations as follows:

$$D_{\Omega}^{p}\eta(\epsilon,\Omega) + \frac{\partial^5\eta(\epsilon,\Omega)}{\partial\epsilon^5} - \eta(\epsilon,\Omega)\frac{\partial^3\eta(\epsilon,\Omega)}{\partial\epsilon^3} + \eta(\epsilon,\Omega)\frac{\partial\eta(\epsilon,\Omega)}{\partial\epsilon} = 0, \quad \text{where} \quad 0 < p \leq 1, \tag{4.19}$$

with the initial condition:

$$\eta(\epsilon, 0) = e^{\epsilon}, \tag{4.20}$$

and exact solution

$$\eta(\epsilon, \Omega) = e^{\epsilon-\Omega}.$$

After applying AT to Eq (4.19), Eq (4.20) is used to obtain:

$$\begin{aligned}\eta(\epsilon, s) - \frac{e^{\epsilon}}{s^2} + \frac{1}{s^p}\Big[\frac{\partial^5 \eta(\epsilon, s)}{\partial \epsilon^5}\Big] - \frac{1}{s^p} A_{\Omega}\Big[A_{\Omega}^{-1}\eta(\epsilon, s) \times \frac{\partial^3 A_{\Omega}^{-1}\eta(\epsilon, s)}{\partial \epsilon^3}\Big] \\ + \frac{1}{s^p} A_{\Omega}\Big[A_{\Omega}^{-1}\eta(\epsilon, s) \times \frac{\partial A_{\Omega}^{-1}\eta(\epsilon, s)}{\partial \epsilon}\Big] = 0.\end{aligned} \tag{4.21}$$

Therefore, the k^{th}-truncated term series is:

$$\eta(\epsilon, s) = \frac{e^{\epsilon}}{s^2} + \sum_{r=1}^{k} \frac{f_r(\epsilon, s)}{s^{rp+1}}, \quad r = 1, 2, 3, 4 \cdots . \tag{4.22}$$

Following is the RAF:

$$\begin{aligned}A_{\Omega} Res(\epsilon, s) = \eta(\epsilon, s) - \frac{e^{\epsilon}}{s^2} + \frac{1}{s^p}\Big[\frac{\partial^5 \eta(\epsilon, s)}{\partial \epsilon^5}\Big] - \frac{1}{s^p} A_{\Omega}\Big[A_{\Omega}^{-1}\eta(\epsilon, s) \times \frac{\partial^3 A_{\Omega}^{-1}\eta(\epsilon, s)}{\partial \epsilon^3}\Big] \\ + \frac{1}{s^p} A_{\Omega}\Big[A_{\Omega}^{-1}\eta(\epsilon, s) \times \frac{\partial A_{\Omega}^{-1}\eta(\epsilon, s)}{\partial \epsilon}\Big] = 0,\end{aligned} \tag{4.23}$$

and the k^{th}-RAFs is:

$$\begin{aligned}A_{\Omega} Res_k(\epsilon, s) = \eta_k(\epsilon, s) - \frac{e^{\epsilon}}{s^2} + \frac{1}{s^p}\Big[\frac{\partial^5 \eta_k(\epsilon, s)}{\partial \epsilon^5}\Big] - \frac{1}{s^p} A_{\Omega}\Big[A_{\Omega}^{-1}\eta_k(\epsilon, s) \times \frac{\partial^3 A_{\Omega}^{-1}\eta_k(\epsilon, s)}{\partial \epsilon^3}\Big] \\ + \frac{1}{s^p} A_{\Omega}\Big[A_{\Omega}^{-1}\eta_k(\epsilon, s) \times \frac{\partial A_{\Omega}^{-1}\eta_k(\epsilon, s)}{\partial \epsilon}\Big] = 0.\end{aligned} \tag{4.24}$$

It takes some calculation to find $f_r(\epsilon, s)$ for $r = 1, 2, 3, ...$ Using these procedures, we replace the r^{th}-truncated series Eq (4.22) for the r^{th}-RAF Eq (4.24), applying $\lim_{s\to\infty}(s^{rp+1})$ and solving $A_{\Omega} Res_{\eta,r}(\epsilon, s)) = 0$, for $r = 1, 2, 3, \cdots$.

$$f_1(\epsilon, s) = -e^{\epsilon}, \tag{4.25}$$

$$f_2(\epsilon, s) = e^{\epsilon}, \tag{4.26}$$

$$f_2(\epsilon, s) = -e^{\epsilon}, \tag{4.27}$$

and so on.

For $r = 1, 2, 3, \cdots$, replace $f_r(\epsilon, s)$ in Eq (4.22):

$$\eta(\epsilon, s) = \frac{e^{\epsilon}}{s} - \frac{e^{\epsilon}}{s^{p+1}} + \frac{e^{\epsilon}}{s^{2p+1}} - \frac{e^{\epsilon}}{s^{3p+1}} + \cdots . \tag{4.28}$$

Apply AIT to obtain:

$$\eta(\epsilon, \Omega) = e^{\epsilon} - \frac{e^{\epsilon}\Omega^{p}}{\Gamma(p+1)} + \frac{e^{\epsilon}\Omega^{2p}}{\Gamma(2p+1)} - \frac{e^{\epsilon}\Omega^{4p}}{\Gamma(3p+1)} + \cdots . \tag{4.29}$$

Figure 7 explores the fractional order comparison using ARPSM for an extended range of p values ($p = 0.33, 0.55, 0.77, 1.00$), providing a more comprehensive analysis of how different orders affect the solution. Figure 8 offers 2D and 3D graphs for ARPSM solutions, further highlighting the changes in solution behavior as the fractional order varies.

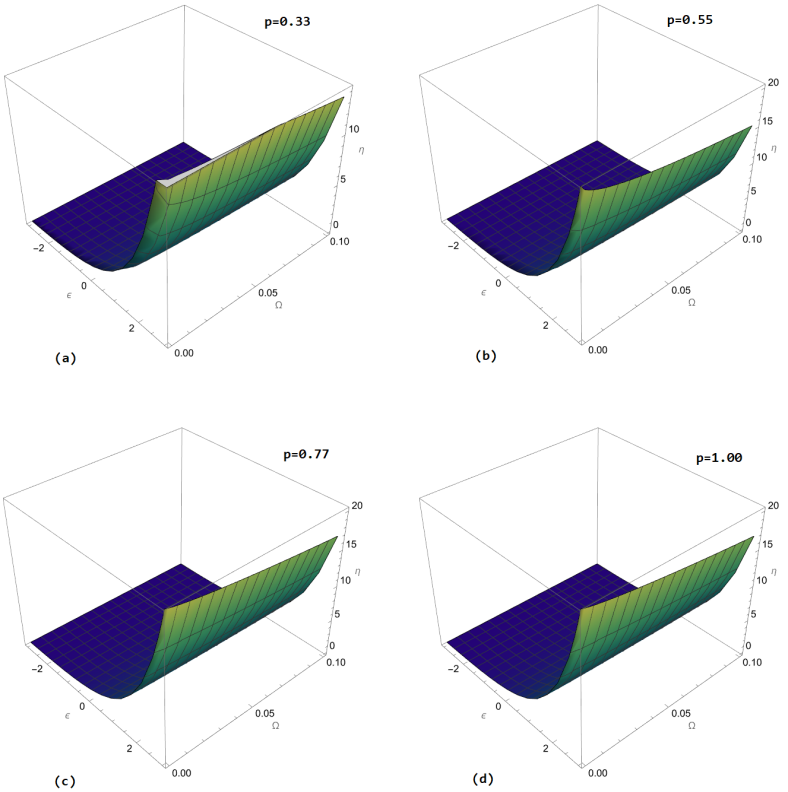

Figure 7. Fractional order comparison using ARPSM for $p = 0.33, 0.55, 0.77, 1.00$.

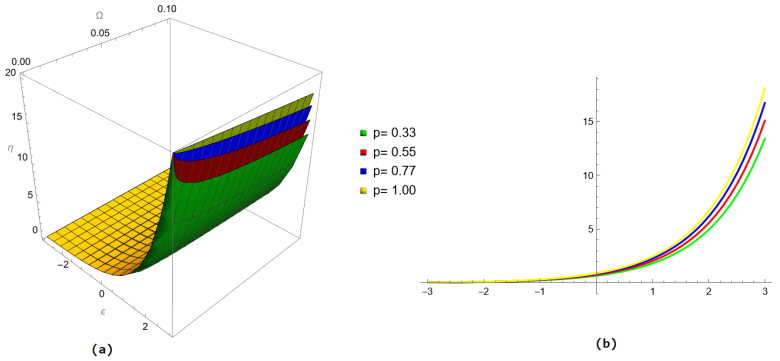

Figure 8. 2D and 3D graphs for comparing ARPSM solution for $p = 0.33, 0.55, 0.77, 1.00$.

4.4. Example 2 using ATIM

Examine the famous fifth-order KdV equations as follows:

$$D^p_\Omega \eta(\epsilon,\Omega) = -\frac{\partial^5 \eta(\epsilon,\Omega)}{\partial \epsilon^5} + \eta(\epsilon,\Omega)\frac{\partial^3 \eta(\epsilon,\Omega)}{\partial \epsilon^3} - \eta(\epsilon,\Omega)\frac{\partial \eta(\epsilon,\Omega)}{\partial \epsilon}, \quad \text{where} \quad 0 < p \leq 1, \tag{4.30}$$

with the initial condition:

$$\eta(\epsilon,0) = e^{\epsilon}, \tag{4.31}$$

and exact solution

$$\eta(\epsilon,\Omega) = e^{\epsilon-\Omega}.$$

Apply AT on either side of Eq (4.30) to obtain:

$$A[D^p_\Omega \eta(\epsilon,\Omega)] = \frac{1}{s^p}\Big(\sum_{k=0}^{m-1}\frac{\eta^{(k)}(\epsilon,0)}{s^{2-p+k}} + A\Big[-\frac{\partial^5 \eta(\epsilon,\Omega)}{\partial \epsilon^5} + \eta(\epsilon,\Omega)\frac{\partial^3 \eta(\epsilon,\Omega)}{\partial \epsilon^3} - \eta(\epsilon,\Omega)\frac{\partial \eta(\epsilon,\Omega)}{\partial \epsilon}\Big]\Big). \tag{4.32}$$

Apply AIT on either side of Eq (4.32) to obtain:

$$\eta(\epsilon,\Omega) = A^{-1}\Big[\frac{1}{s^p}\Big(\sum_{k=0}^{m-1}\frac{\eta^{(k)}(\epsilon,0)}{s^{2-p+k}} + A\Big[-\frac{\partial^5 \eta(\epsilon,\Omega)}{\partial \epsilon^5} + \eta(\epsilon,\Omega)\frac{\partial^3 \eta(\epsilon,\Omega)}{\partial \epsilon^3} - \eta(\epsilon,\Omega)\frac{\partial \eta(\epsilon,\Omega)}{\partial \epsilon}\Big]\Big)\Big]. \tag{4.33}$$

Iteratively apply the AT to obtain:

$$\begin{aligned}\eta_0(\epsilon,\Omega) =& A^{-1}\Big[\frac{1}{s^p}\Big(\sum_{k=0}^{m-1}\frac{\eta^{(k)}(\epsilon,0)}{s^{2-p+k}}\Big)\Big]\\ =& A^{-1}\Big[\frac{\eta(\epsilon,0)}{s^2}\Big]\\ =& e^{\epsilon}.\end{aligned}$$

Applying Riemann-Liouville integral on Eq (4.19),

$$\eta(\epsilon,\Omega) = e^{\epsilon} - A\Big[-\frac{\partial^5 \eta(\epsilon,\Omega)}{\partial \epsilon^5} + \eta(\epsilon,\Omega)\frac{\partial^3 \eta(\epsilon,\Omega)}{\partial \epsilon^3} - \eta(\epsilon,\Omega)\frac{\partial \eta(\epsilon,\Omega)}{\partial \epsilon}\Big]. \tag{4.34}$$

The use of the ATIM technique provides the following terms:

$$\begin{aligned}\eta_0(\epsilon,\Omega) &= e^{\epsilon},\\ \eta_1(\epsilon,\Omega) &= -\frac{e^{\epsilon}\Omega^p}{\Gamma(p+1)},\\ \eta_2(\epsilon,\Omega) &= \frac{e^{\epsilon}\Omega^{2p}}{\Gamma(2p+1)},\\ \eta_3(\epsilon,\Omega) &= -\frac{e^{\epsilon}\Omega^{3p}}{\Gamma(3p+1)}.\end{aligned} \tag{4.35}$$

The final solution that is obtained via ATIM is given as:

$$\eta(\epsilon, \Omega) = \eta_0(\epsilon, \Omega) + \eta_1(\epsilon, \Omega) + \eta_2(\epsilon, \Omega) + \eta_3(\epsilon, \Omega) + \cdots . \tag{4.36}$$

$$\eta(\epsilon, \Omega) = e^{\epsilon}\left(1 - \frac{\Omega^p}{\Gamma(p+1)} + \frac{\Omega^{2p}}{\Gamma(2p+1)} - \frac{\Omega^{4p}}{\Gamma(3p+1)} + \cdots\right). \tag{4.37}$$

Table 4 analyzes the effect of various fractional orders for ARPSM and ATIM, for Example 2, indicating the consistency and accuracy of both methods across different fractional orders. Figures 9 and 10 continue the analysis for ATIM, comparing fractional order solutions and offering 3D and 2D views further to elucidate the complex behavior of fractional wave systems as modeled by the Kawahara and KdV equations. These figures and tables collectively emphasize the efficacy of ARPSM and ATIM in providing accurate and insightful solutions for fractional nonlinear PDEs, especially in the context of nonlinear wave phenomena in applied mathematics and physics. The graphical representations and error comparisons showcase the reliability and precision of these methods in solving complex fractional models.

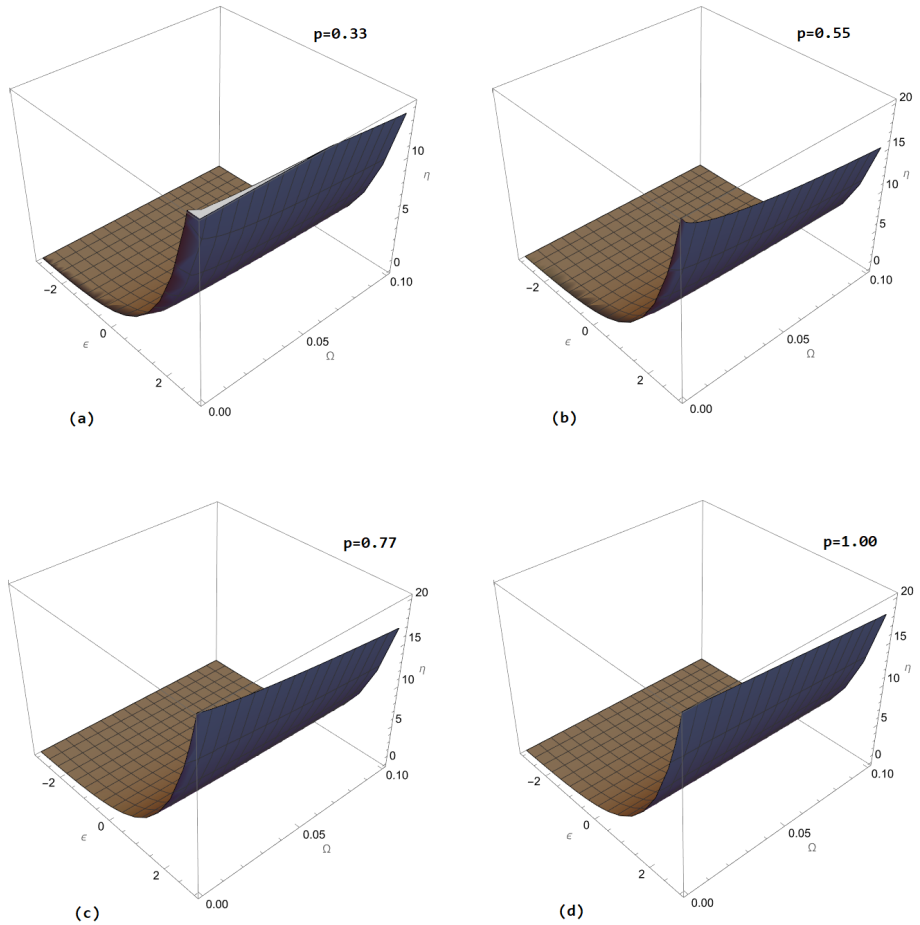

Figure 9. Fractional order comparison using ATIM for $p = 0.33, 0.55, 0.77, 1.00$.

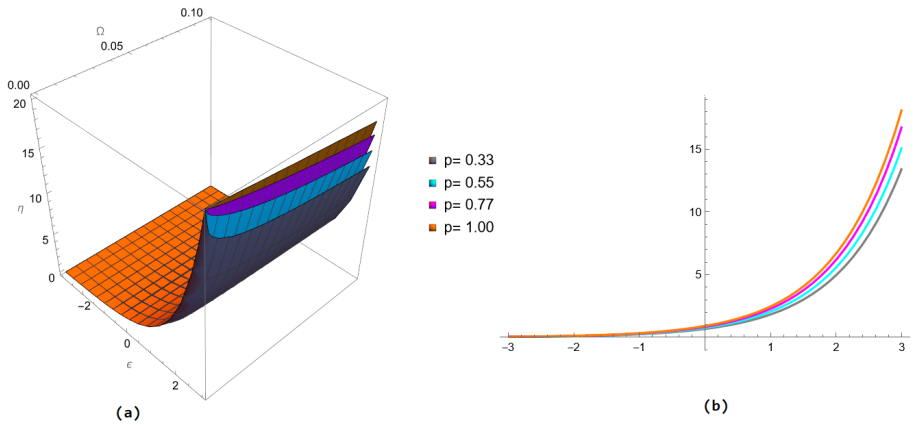

Figure 10. Fractional order 3D and 2D comparison using ATIM for $p = 0.33, 0.55, 0.77, 1.00$.

Table 4. Analysis of various fractional order of ARPSM and ATIM of Example 2 for $\Omega = 0.1$.

ϵ	$ARPSM\ ATIM$ $p = 0.55$	$ARPSM\ ATIM$ $p = 0.77$	$ARPSM\ ATIM$ $p = 1.00$	$Exact$	$Error_{p=1.0}$
1.0	2.49168	2.63507	2.69123	2.69123	4.473861×10^{-7}
1.1	2.75373	2.91220	2.97427	2.97427	4.944381×10^{-7}
1.2	3.04335	3.21848	3.28708	3.28708	5.464386×10^{-7}
1.3	3.36342	3.55697	3.63279	3.63279	6.039081×10^{-7}
1.4	3.71715	3.93106	4.01485	4.01485	6.674217×10^{-7}
1.5	4.10809	4.34449	4.43710	4.43710	7.376150×10^{-7}
1.6	4.54014	4.80141	4.90375	4.90375	8.151907×10^{-7}
1.7	5.01763	5.30638	5.41948	5.41948	9.009250×10^{-7}
1.8	5.54534	5.86445	5.98945	5.98945	9.956761×10^{-7}
1.9	6.12855	6.48122	6.61937	6.61937	1.100392×10^{-6}
2.0	6.77309	7.16286	7.31553	7.31553	1.216121×10^{-6}

The study utilizes advanced analytical methods, precisely the ARPSM and the ATIM, to investigate the fractional Kawahara and fifth-order KdV equations. The discussion of figures and tables highlights the effectiveness of these methods in providing accurate approximate solutions, comparing their results with exact solutions, and examining the effects of fractional orders on the solutions.

5. Conclusions

In conclusion, our analytical investigation into the fractional Kawahara equation and fifth-order KdV equations employing the ARPSM and ATIM has yielded significant insights and advancements in understanding nonlinear wave phenomena. Through rigorous analysis and computational simulations, we have demonstrated the effectiveness of these advanced analytical techniques in providing accurate and insightful solutions to these complex equations governed by fractional calculus under the Caputo operator framework. Our findings contribute to the theoretical understanding of nonlinear wave

dynamics and offer practical analytical tools for addressing complex mathematical models in various scientific and engineering domains. Further research in this direction holds promise for exploring additional applications of the Aboodh methods and advancing our understanding of nonlinear wave phenomena in diverse real-world contexts. Future research can extend the ARPSM and ATIM methods to more complex nonlinear fractional PDEs, including those with higher-order fractional operators. Exploring their application to multidimensional systems could provide deeper insights into wave propagation in fields like quantum field theory. Investigating computational efficiency and convergence across different fractional orders may optimize these techniques for broader use. Applying these methods to real-world engineering problems could further validate their utility in practical settings.

Author contributions

Conceptualization, M.Y.A.; Data curation, H.A.; Formal analysis, M.Y.A; Resources, H.A.; Investigation, M.Y.A.; Project administration, M.Y.A.; Validation, H.A.; Software, H.A.; Validation, M.Y.A.; Visualization, M.Y.A.; Validation, H.A.; Visualization, M.Y.A.; Resources, H.A.; Project administration, H.A.; Writing-review & editing, H.A.; Funding, M.Y.A. All authors have read and agreed to the published version of the manuscript.

Acknowledgments

The authors gratefully acknowledge the funding of the Deanship of Graduate Studies and Scientific Research, Jazan University, Saudi Arabia, through project number: RG24-L02.

Conflict of interest

The authors declare that they have no conflicts of interest.

References

1. R. Khalil, M. Al Horani, A. Yousef, M. Sababheh, A new definition of fractional derivative, *J. Comput. Appl. Math.*, **264** (2014), 65–70. https://doi.org/10.1016/j.cam.2014.01.002
2. S. Khirsariya, S. Rao, J. Chauhan, Solution of fractional modified Kawahara equation: a semi-analytic approach, *Math. Appl. Sci. Eng.*, **4** (2023), 249–350. https://doi.org/10.5206/mase/16369
3. S. R. Khirsariya, J. P. Chauhan, S. B. Rao, A robust computational analysis of residual power series involving general transform to solve fractional differential equations, *Math. Comput. Simul.*, **216** (2024), 168–186. https://doi.org/10.1016/j.matcom.2023.09.007
4. S. R. Khirsariya, S. B. Rao, J. P. Chauhan, Semi-analytic solution of time-fractional Korteweg-de Vries equation using fractional residual power series method, *Results Nonlinear Anal.*, **5** (2022), 222–234.
5. L. K. B. Kuroda, A. V. Gomes, R. Tavoni, P. F. de Arruda Mancera, N. Varalta, R. de Figueiredo Camargo, Unexpected behavior of Caputo fractional derivative, *Comp. Appl. Math.*, **36** (2017), 1173–1183. https://doi.org/10.1007/s40314-015-0301-9

6. R. Almeida, N. Bastos, M. Teresa, T. Monteiro, A prelude to the fractional calculus applied to tumor dynamic, *Math. Methods Appl. Sci.*, **39** (2016), 4846–4855.
7. J. Losada, J. J. Nieto, Properties of a new fractional derivative without singular kernel, *Progr. Fract. Differ. Appl.*, **1** (2015), 87–92.
8. M. Caputo, M. Fabrizio, A new definition of fractional derivative without singular kernel, *Progr. Fract. Differ. Appl.*, **1** (2015), 73–85.
9. S. Alshammari, M. M. Al-Sawalha, R. Shah, Approximate analytical methods for a fractional-order nonlinear system of Jaulent–Miodek equation with energy-dependent Schrodinger potential, *Fractal Fract.*, **7** (2023), 140. https://doi.org/10.3390/fractalfract7020140
10. A. Atangana, J. F. Gomez-Aguilar, A new derivative with normal distribution kernel: theory, methods and applications. *Phys. A: Stat. Mech. Appl.*, **476** (2017), 1–14. https://doi.org/10.1016/j.physa.2017.02.016
11. M. Alesemi, N. Iqbal, M. S. Abdo, Novel investigation of fractional-order Cauchy-reaction diffusion equation involving Caputo-Fabrizio operator, *J. Funct. Spaces*, **2022** (2022), 1–14. https://doi.org/10.1155/2022/4284060
12. N. Iqbal, H. Yasmin, A. Rezaiguia, J. Kafle, A. O. Almatroud, T. S. Hassan, Analysis of the fractional-order Kaup-Kupershmidt equation via novel transforms, *J. Math.*, **2021** (2021), 1–13. https://doi.org/10.1155/2021/2567927
13. N. Iqbal, H. Yasmin, A. Ali, A. Bariq, M. M. Al-Sawalha, W. W. Mohammed, Numerical methods for fractional-order Fornberg-Whitham equations in the sense of Atangana-Baleanu derivative, *J. Funct. Spaces*, **2021** (2021), 1–10. https://doi.org/10.1155/2021/2197247
14. P. Sunthrayuth, A. M. Zidan, S. W. Yao, R. Shah, M. Inc, The comparative study for solving fractional-order Fornberg-Whitham equation via ρ-Laplace transform, *Symmetry*, **13** (2021), 784. https://doi.org/10.3390/sym13050784
15. T. Kakutani, H. Ono, Weak non-linear hydromagnetic waves in a cold collision-free plasma, *J. Phys. Soc. Jpn.*, **26** (1969), 1305–1318. https://doi.org/10.1143/JPSJ.26.1305
16. R. Shah, H. Khan, D. Baleanu, P. Kumam, M. Arif, A novel method for the analytical solution of fractional Zakharov-Kuznetsov equations, *Adv. Differ. Equ.*, **2019** (2019), 1–14. https://doi.org/10.1186/s13662-019-2441-5
17. A. Goswami, J. Singh, D. Kumar, Numerical simulation of fifth order KdV equations occurring in magneto-acoustic waves, *Ain Shams Eng. J.*, **9** (2018), 2265–2273. https://doi.org/10.1016/j.asej.2017.03.004
18. M. O. Miansari, M. E. Miansari, A. Barari, D. D. Ganji, Application of He's variational iteration method to nonlinear Helmholtz and fifth-order KdV equations, *J. Appl. Math., Stat. Inf. (JAMSI)*, **5** (2009).
19. S. Abbasbandy, F. S. Zakaria, Soliton solutions for the fifth-order KdV equation with the homotopy analysis method. *Nonlinear Dyn.*, **51** (2008), 83–87. https://doi.org/10.1007/s11071-006-9193-y
20. A. M. Wazwaz, Solitons and periodic solutions for the fifth-order KdV equation, *Appl. Math. Lett.*, **19** (2006), 1162–1167. https://doi.org/10.1016/j.aml.2005.07.014

21. M. T. Darvishi, F. Khani, Numerical and explicit solutions of the fifth-order Korteweg-de Vries equations, *Chaos, Solitons Fract.*, **39** (2009), 2484–2490. https://doi.org/10.1016/j.chaos.2007.07.034
22. I. Ahmad, H. Seno, An epidemic dynamics model with limited isolation capacity, *Theory Biosci.*, **142** (2023), 259–273. https://doi.org/10.1007/s12064-023-00399-9
23. H. Khan, R. Shah, P. Kumam, D. Baleanu, M. Arif, Laplace decomposition for solving nonlinear system of fractional order partial differential equations, *Adv. Differ. Equ.*, **2020** (2020), 1–18. https://doi.org/10.1186/s13662-020-02839-y
24. S. Zhang, Application of Exp-function method to a KdV equation with variable coefficients, *Phys. Lett. A*, **365** (2007), 448–453. https://doi.org/10.1016/j.physleta.2007.02.004
25. O. A. Arqub, Series solution of fuzzy differential equations under strongly generalized differentiability, *J. Adv. Res. Appl. Math.*, **5** (2013), 31–52.
26. O. Abu Arqub, Z. Abo-Hammour, R. Al-Badarneh, S. Momani, A reliable analytical method for solving higher-order initial value problems, *Discrete Dyn. Nat. Soc.*, **2013** (2013), 673829. https://doi.org/10.1155/2013/673829
27. J. Zhang, Z. Wei, L. Li, C. Zhou, Least-squares residual power series method for the time-fractional differential equations, *Complexity*, **2019** (2019), 1–15. https://doi.org/10.1155/2019/6159024
28. I. Jaradat, M. Alquran, R. Abdel-Muhsen, An analytical framework of 2D diffusion, wave-like, telegraph, and Burgers' models with twofold Caputo derivatives ordering, *Nonlinear Dyn.*, **93** (2018), 1911–1922. https://doi.org/10.1007/s11071-018-4297-8
29. Y. Xie, I. Ahmad, T. I. S. Ikpe, E. F. Sofia, H. Seno, What influence could the acceptance of visitors cause on the epidemic dynamics of a reinfectious disease?: a mathematical model, *Acta Biotheor.,* **72** (2024), 3. https://doi.org/10.1007/s10441-024-09478-w
30. S. Mukhtar, M. Sohaib, I. Ahmad, A numerical approach to solve volume-based batch crystallization model with fines dissolution unit, *Processes*, **7** (2019), 453. https://doi.org/10.3390/pr7070453
31. M. F. Zhang, Y. Q. Liu, X. S. Zhou, Efficient homotopy perturbation method for fractional nonlinear equations using Sumudu transform, *Therm. Sci.*, **19** (2015), 1167–1171.
32. M. I. Liaqat, S. Etemad, S. Rezapour, C. Park, A novel analytical Aboodh residual power series method for solving linear and nonlinear time-fractional partial differential equations with variable coefficients, *AIMS Math.*, **7** (2022), 16917–16948. https://doi.org/10.3934/math.2022929
33. M. I. Liaqat, A. Akgul, H. Abu-Zinadah, Analytical investigation of some time-fractional Black-Scholes models by the Aboodh residual power series method, *Mathematics*, **11** (2023), 276. https://doi.org/10.3390/math11020276
34. G. O. Ojo, N. I. Mahmudov, Aboodh transform iterative method for spatial diffusion of a biological population with fractional-order, *Mathematics*, **9** (2021), 155. https://doi.org/10.3390/math9020155
35. M. A. Awuya, G. O. Ojo, N. I. Mahmudov, Solution of space-time fractional differential equations using Aboodh transform iterative method, *J. Math.*, **2022** (2022), 4861588. https://doi.org/10.1155/2022/4861588

36. M. A. Awuya, D. Subasi, Aboodh transform iterative method for solving fractional partial differential equation with Mittag-Leffler kernel, *Symmetry*, **13** (2021), 2055. https://doi.org/10.3390/sym13112055

37. K. S. Aboodh, The new integral transform'Aboodh transform, *Global J. Pure Appl. Math.*, **9** (2013), 35–43.

38. S. Aggarwal, R. Chauhan, A comparative study of Mohand and Aboodh transforms, *Int. J. Res. Adv. Technol.*, **7** (2019), 520–529.

39. M. E. Benattia, K. Belghaba, Application of the Aboodh transform for solving fractional delay differential equations, *Univ. J. Math. Appl.*, **3** (2020), 93–101. https://doi.org/10.32323/ujma.702033

40. B. B. Delgado, J. E. Macias-Diaz, On the general solutions of some non-homogeneous Div-curl systems with Riemann-Liouville and Caputo fractional derivatives, *Fractal Fract.*, **5** (2021), 117. https://doi.org/10.3390/fractalfract5030117

41. S. Alshammari, M. Al-Smadi, I. Hashim, M. A. Alias, Residual power series technique for simulating fractional Bagley-Torvik problems emerging in applied physics, *Appl. Sci.*, **9** (2019), 5029. https://doi.org/10.3390/app9235029

AIMS Press